ISSN 1063-7796, Physics of Particles and Nuclei, 2016, Vol. 47, No. 4, pp. 681–701. © Pleiades Publishing, Ltd., 2016.
Original Russian Text © N.A. Gundorin, Sh.S. Zeinalov, Yu.N. Kopach, A.B. Popov, V.I. Furman, 2016, published in Fizika Elementarnykh Chastits i Atomnogo Yadra, 2016, Vol. 47, No. 4.

Investigations of Fission Characteristics and Correlation Effects

N. A. Gundorin, Sh. S. Zeinalov, Yu. N. Kopach, A. B. Popov*, and V. I. Furman

Joint Institute for Nuclear Research, Dubna, Moscow region, 141980 Russia

**e-mail: popov_ab@nf.jinr.ru*

Abstract—We review the experimental results on the *P*-even and *P*-odd angular correlations of fission fragments in the fission of the ^{235}U and ^{239}Pu nuclei induced by unpolarized and polarized resonance neutrons, and on the TRI and ROT effects in the ternary and binary fission of actinides induced by polarized thermal neutrons. Also reported are the measured yields of prompt and delayed neutrons per fission event. The experimental data are analyzed within a novel theoretical framework developed by the JINR—RNC KI Collaboration, whereby the reduction of the multidimensional phase space of fission fragments to the $J\pi K$-channel space is consistently validated and the role of resonance interference in the observed correlation effects is revealed.

DOI: 10.1134/S1063779616040079

1. INTRODUCTION

The fission of atomic nuclei discovered in 1938 by O. Hahn and F. Strassmann, who published their results on January 6, 1939, had enormous and primarily tragic implications for mankind: hundreds of thousands of civilians were killed by the US nuclear bombardment of Hiroshima and Nagasaki on August 6 and 9, 1945. Nuclear weapons of various types were massively produced since then, and the accumulated arsenal is capable of reducing the planet to ashes. Just how precarious the very existence of our civilization is escapes the laymen's comprehension. The negative connotations of the discovery of nuclear fission are partially mitigated by successful applications in such peaceful areas as energy generation, transport, technology, and medicine.

Naturally, the characteristics of nuclear fission and the properties of various nuclei revealed in neutron-induced fission were extensively investigated for several decades after the discovery of the fission phenomenon. A huge database has been accumulated on the fission cross sections and their interrelations with those of neutron capture, the energy balance in an individual fission event, the multiplicity of neutrons emitted in nuclear fission, and other characteristics relevant to designing and reliably operating the nuclear facilities. However, nuclear fission in itself proved to be so complex and intriguing that both the experimental and theoretical investigations of this phenomenon are still carrying on.

Ever since the operation of the IBR-1 pulsed reactor was commissioned in 1960 in the Laboratory of Neutron Physics, the physics of nuclear fission has been intensively investigated toward obtaining the data of either the fundamental and applied interest. During the last operation decade of the neutron source IBR-30 + LUE40 (shut down in 2001 upon exhausting the resource of the booster breeding zone) the *P*-even and *P*-odd angular correlations of fragments in the fission of ^{235}U and ^{239}Pu induced by polarized resonance neutrons with energies up to 30 eV were investigated in a unique series of experiments [1–10] in collaboration with PINP (Gatchina), and the asymmetry of fragment emission in the fission of aligned ^{235}U nuclei induced by unpolarized neutrons in the same energy range was measured [11, 12] in collaboration with IPPE (Institute of Physics and Power Engineering, Obninsk). We owe these results to the LNP JINR source of resonance neutrons with record intensity and energy resolution that allowed us to investigate a number of compound states of the target nucleus, as well as to an efficient system for polarizing the resonance neutrons by passing them through a polarized hydrogen target as earlier conceived by F.L. Shapiro [13].

Developed during the same years was a consistent theory of binary fission [14–16] based on the helicity representation for describing the binary channels of fission, as proposed by V.M. Strutinskii [17]. This multichannel and multilevel *S*-matrix theory allows reduction of the multidimensional ($\sim 10^9$ degrees of freedom) phase space of fission fragments to the $J^{\pi}K$ effective-channel space heuristically introduced by A. Bohr [18], where J is the spin of the fissile nucleus, K is its projection to the deformation axis, and π is the spatial parity. Strutinskii's approach was developed in parallel with Bohr's hypothesis, but was not properly recognized because the original treatment was restricted to total cross sections and did not include the interference between the reaction amplitudes, which is essential for describing the angular distribu-

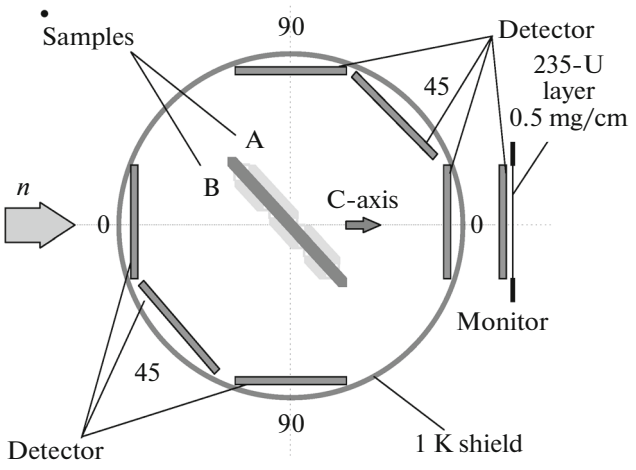

Fig. 1. The layout of the experiment for measuring the fragment anisotropy in neutron-induced fission of the aligned ^{235}U nuclei.

tions of fission fragments. In [15, 16], the helicity representation with definite parity for the fission-fragment channels was developed and then employed for deriving the differential cross section of the (n,f) reaction in the standard Blatt—Biedenharn form [19]. Using the description [20] of the transitional-state wave function in the fission channel, the obtained differential cross section could then be summed over all fragment states relevant to a given fission mode so as to reproduce the experimentally measured cross section.

As a result, the dynamics of the fission reaction was described in terms of a reduced S-matrix in the $J\pi K$ effective-channel space with a limited number of degrees of freedom. Thereby, the validity of Bohr's hypothesis [18] was substantiated, and the fission cross sections were formulated for a quantitative analysis of the data. The analysis was based on a multilevel multichannel resonant parametrization of the reduced S-matrix with the partial amplitudes for the fission and neutron widths parametrized using standard real phase shifts, which allow to consistently account for the interlevel interference in the differential and total cross sections of the (n,f) reaction.

Note that the helicity operator does not commute with that of the fragments' orbital momentum. Therefore, the helicity quantum number is not strictly conserved at the rupture point of the fissile nucleus where the formation of fragments in nonadiabatic. However, the proposed formalism proved to be sufficiently accurate [14, 15] because the centrifugal energy is small compared to the total kinetic energy of the fragments. The estimates [14, 15] of the uncertainty arising from using the helicity representation directly at the rupture point have been confirmed by the results of recent investigations of the so-called TRI and ROT effects in ternary and binary fission induced by polarized thermal neutrons (see Section 3 below).

On the whole, the theoretical formalism [14–16] provided a consistent description of all correlation effects in nuclear fission that have been observed during the last 15 years.

2. THE ANISOTROPY OF FRAGMENT EMISSION AND THE P-EVEN AND P-ODD EFFECTS

Angular Anisotropy of Fission Fragments

Shown in Fig. 1 is the schematic layout of the samples and detectors in the experiments [11, 12] with the ^{235}U nuclei aligned by the hyperfine interaction of the electric quadrupole moment of the uranium nucleus with the electric-field gradient of the uranyl ion (UO_2) in the form of a monocrystal of uranyl—rubidium nitrate cooled to ~0.15K. The silicon detectors were operated at 1K. A ^{3}He-^{4}He dilution refrigerator in continuous operation has been used.

The number of events detected by the counter placed at polar angle θ for the target temperature T may be put down as

$$N(E_n,T) = I(E_n,\Omega)[1 + A_2(E_n)f_2(T)P_2(\cos\theta)], \quad (1)$$

where $I(E_n,\Omega)$ is the normalization coefficient depending on the neutron-beam intensity and on the solid angle subtended by the detector, $f_2(T)$ is the alignment of uranium nuclei in the target, and

$$A_2 = \frac{15I^2}{\sqrt{(2I-1)I(I+1)(2I-3)}}\frac{\sigma_{nf2}}{\sigma_{nf0}}, \quad (2)$$

where the cross sections

$$\sigma_{nf0}(E_n) = \pi\lambda^2\sum_J g_J\sum_K\left|S_J\left(0\tfrac{1}{2}\to Kf\right)\right|^2, \quad (3)$$

$$\sigma_{nf2}(E_n) = \pi\lambda^2\sum_{JJ'}\sqrt{g_Jg_{J'}}U\left(\tfrac{1}{2}IJ'2;JI\right) \times\sum_K C^{JK}_{JK20}S^*_{J'}\left(0\tfrac{1}{2}\to Kf\right)S_J\left(0\tfrac{1}{2}\to Kf\right) \quad (4)$$

include the interference between the resonances in contrast with earlier treatments [21]. The experimental data were analyzed using the total neutron cross sections and the total and spin-separated cross sections for the fission of ^{235}U compiled in the database NNDC [22]. The quantity $A_2(E_n)$ was fitted using the cross-section data, and a satisfactory description of all available data was reached. The fit yielded a new set of resonance parameters including the partial fission widths $\Gamma_f^{J\pi K}$. It was initially assumed that three channels are open for the resonances with spin $J = 3$ ($K = 0$, $K = 1$, $K = 2$), and two channels are open for those with $J = 4$ ($K = 1, K = 2$). In agreement with the simplest version of Bohr's hypothesis, the states

with $J^{\pi}K = 4^{-}0$ were assumed to be forbidden. The channels with $K > 2$ were not taken into account since they should have higher fission barriers and, moreover, for them the geometric factors determining the anisotropy coefficient are positive whereas the observed $A_2(E_n)$ values are negative throughout the investigated energy range. The integral distributions of partial fission widths for the resonances with $J^{\pi} = 4^{-}$ obtained in this analysis failed to agree with the Porter—Thomas form. The latter suggested that the channel $J^{\pi}K = 4^{-}0$ should also be considered for the resonances with $J^{\pi} = 4^{-}$. The existence of such channels was theoretically predicted in [23] where, in addition to the $J^{\pi}K$ characteristics of fission barriers, the signature quantum numbers s and r related to the symmetry of the first and second fission barriers were introduced. Upon including the $J^{\pi}K = 4^{-}0$ channel, the analysis yielded the sets of partial and total fission widths for the two spin states that agree with the Porter—Thomas distributions.

The final fits of the anisotropy factor $A_2(E_n)$ are shown in Fig. 2 together with the total fission cross section. Relative contributions of different K components to the total and spin-separated fission cross sections are shown in Fig. 3. Relative weights of different $J^{\pi}K$ components show strong variation from resonance to resonance. This is because the components with different spin projections K are strongly mixed in the wave functions of compound states of heavy deformed nuclei by the Coriolis force [24, 25]. Phenomenologically, this proves that the statistical nature of the compound-state wave function determines the wave-function amplitude of the transitional state in the fission channel $J^{\pi}K$. In themselves, these states describe the motion of the fissioning nucleus in the "deformation" space until the breakup into fragments (the details may be found in [16, 20]).

It should be noted that the obtained sets of resonance parameters are not unique: the results of the fit of combined experimental data are affected by a particular selection of negative resonances and by including or not the resonances with very small or very large fission widths that play but a small role in the cross-section description. However, the relative contributions of different $J^{\pi}K$ channels averaged over the investigated set of compound states prove to be insensitive to varying the fit conditions, and therefore may be employed for a quantitative analysis of the interference between the s and p resonances.

P-Even and P-Odd Effects in the Angular Distributions of Fission FRagments

The energy dependences of the parity conservation (PC) and parity non-conservation (PNC) effects in the angular asymmetry of fragment emission in nuclear fission induced by resonance neutrons with energies from the near-thermal up to ~ 30 eV were investigated in [1–10]. A beam of polarized neutrons from the pulsed source IBR30+LUE-40 was impinging on multilayer (up to 40 layers) fission chambers with fissile-material content of 2 g of ^{235}U and 0.25 g of ^{239}Pu. In measuring the P-even forward—backward (FB) asymmetry, the fission chamber was oriented along the neutron beam so that the layers of fissile material were normal to the incident neutron momentum. When measuring the P-odd and P-even left—right (LR) effects, the momenta of detected fragments were perpendicular to the axis of the polarized-neutron beam (see Fig. 4). The direction of neutron polarization was periodically varied, and the anisotropy effects were detected using the counts of the fission chamber as in measuring the FB asymmetry. For these measurements, the chamber was oriented so that the target layers were parallel to the neutron beam, and only the sign of neutron polarization was changed. In the measurements of the P-even LR effect, the fissile layers were parallel to spin direction of beam neutrons, whereas in those of the P-odd effect the chamber position was such that neutron spins were perpendicular to the fissile layers. The measurements [1—8] allowed to estimate the asymmetry fac-

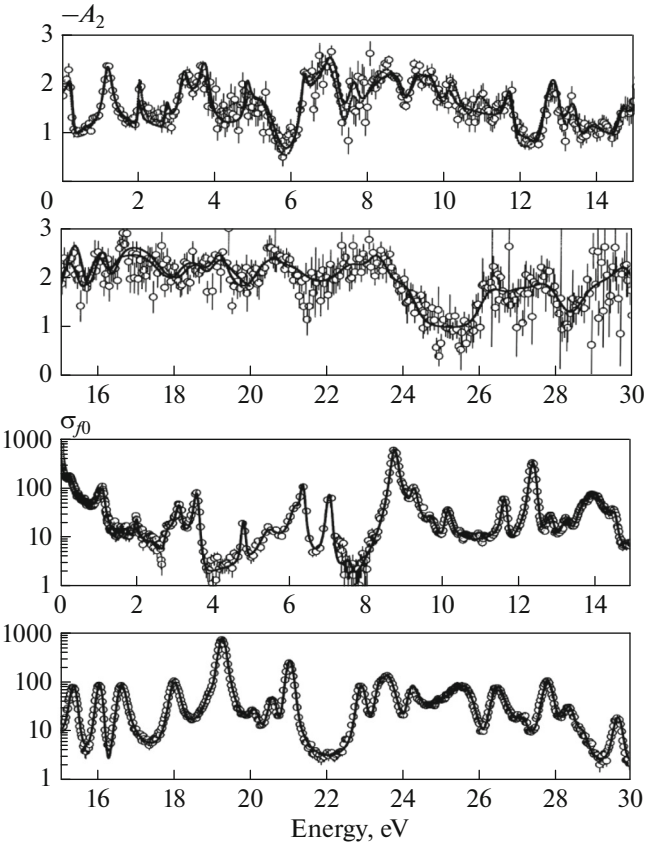

Fig. 2. The fits of the measured values of $A_2(E_n)$ and $\sigma_{f0}(E_n)$.

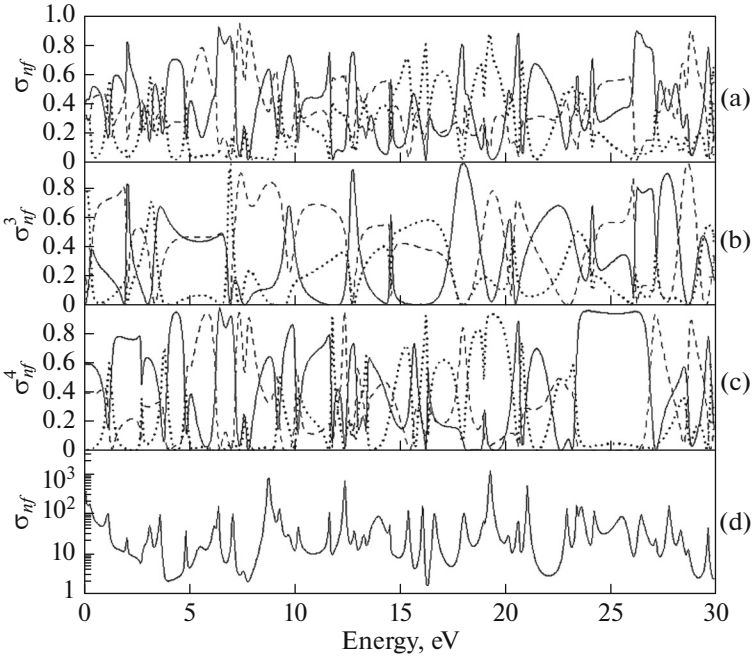

Fig. 3. The decomposition of the total and spin-separated fission cross sections to different K components: $K = 0$ (dotted curves), $K = 1$ (solid curves), and $K = 2$ (dashed curves). The total fission cross section is shown in the bottom panel (d).

tors $\sigma_{\exp}^{FB}(E)$, $\sigma_{\exp}^{LR}(E)$, and $\sigma_{\exp}^{PNC}(E)$ for ^{235}U and ^{239}Pu in the energy range up to ~30 eV.

The parity-conserving differential cross section of the fission process has a form

$$\frac{d\sigma_{nf}(E_n)}{d\Omega} = \frac{1}{4\pi}\Big\{\sigma_{nf}^{(0)}(E_n) + \sigma_{nf}^{FB}(E_n)(\vec{n}_f\vec{n}_k) + p_n\sigma_{nf}^{LR}(E_n)(\vec{n}_f[\vec{n}_k\times\vec{n}_s])\Big\}, \quad (5)$$

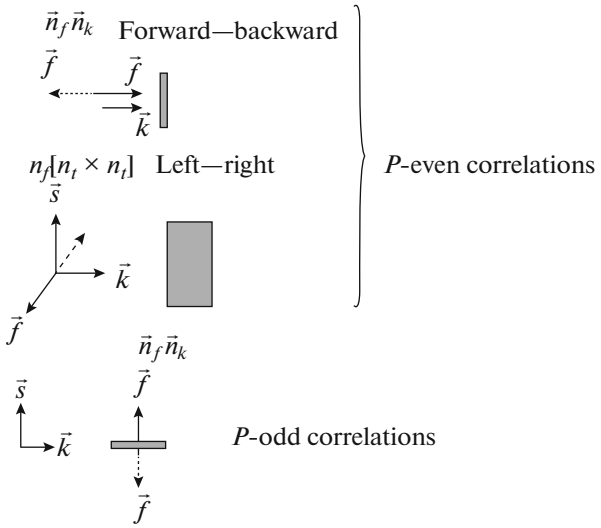

Fig. 4. The schematic view of the directions of momenta for neutrons and fragments and the orientation of neutron polarization in the measurements of the P-even and P-odd angular correlations of fission fragments.

where p_n is the neutron polarization and $\vec{n}_f$, $\vec{n}_k$, $\vec{n}_s$ are the unit vectors along the directions of the (light) fragment, the neutron momentum, and the neutron spin, respectively. The total fission cross section that enters (5) is as follows:

$$\sigma_{nf}^{(0)} = \pi\lambda\!\!\!^{-2}\sum_J g_J\sum_{lj}\sum_{K\geq 0}\sum_{\Pi}|S_J(lj\to K\Pi f)|^2, \quad (6)$$

where l is the neutron orbital momentum, j is the initial-state spin, K is the projection of the compound-nucleus spin J to the axis of the fissioning nucleus, and Π is the parity of the exit fission channel f. The cross section that determines the forward—backward correlations has a form [16]

$$\sigma_{nf}^{FB} = \pi\lambda\!\!\!^{-2}\sum_{J'Jj}\sum_{K\geq 0} q(J'JjK) \times \mathrm{Im}\left[S_{J'}^*(1j\to K-\Pi_0 f)S_J\left(0\tfrac{1}{2}\to K\Pi_0 f\right)\right]. \quad (7)$$

The cross section that describes the left—right anisotropy is expressed as

$$\sigma_{nf}^{LR} = \pi\lambda\!\!\!^{-2}\sum_{J'Jj}(-\beta_j)\sum_{K\geq 0} q(J'JjK) \times \mathrm{Re}\left[S_{J'}^*(1j\to K-\Pi_0 f)S_J\left(0\tfrac{1}{2}\to K\Pi_0 f\right)\right] \quad (8)$$

Here, S is the reduced scattering matrix [16], and the geometric factor has a form

$$q(J'JjK) = \Pi_0\, g_J(-1)^{3/2-j}[6(2j+1)]^{1/2} \times U\left(IjJ1;J'\tfrac{1}{2}\right)C_{JK10}^{J'K}, \quad \beta_{1/2}=1, \quad \beta_{3/2}=-0.5. \quad (9)$$

The cross section that determines the parity-violating effects is written as follows:

$$\sigma_{nf}^{PNC} = \pi\lambda^{-2}\sqrt{3}p_n(\vec{n}_f\vec{n}_s)\Bigg[-\frac{2}{2I+1}\sqrt{\frac{I(I+1)}{3}} \times \sum_{\Pi=\Pi_0,-\Pi_0}\Pi\,\mathrm{Im}\Big\{S^*_{I+1/2}\Big(0\tfrac{1}{2}\to 0-\Pi f\Big) \times S_{I-1/2}\Big(0\tfrac{1}{2}\to 0\Pi f\Big)\Big\} + 2\Pi_0\sum_{JJ'} g_J U\Big(I\tfrac{1}{2}J1;J'\tfrac{1}{2}\Big) \times \sum_{|K|>0} C^{J'|K|}_{J|K|10}\,\mathrm{Im}\Big\{S^*_{J'}\Big(0\tfrac{1}{2}\to|K|-\Pi_0 f\Big) \times S_J\Big(0\tfrac{1}{2}\to|K|\Pi_0 f\Big)\Big\}\Bigg]. \quad (10)$$

Only the channel with $K = 0$ is open in the reaction ^{239}Pu(n, f), and therefore for this case, denoting $S_J\left(0,\frac{1}{2}\to|0|\,\Pi f\right)\equiv S_J$ for convenience, we obtain

$$\sigma^{PNC} = \frac{4\pi}{k^2}\frac{\sqrt{3}}{2}p_n\frac{1}{4} \times \mathrm{Im}\left[\sum_{\nu} S_1^{*PC}S_{0_\nu}^{PNC} - \sum_{\nu} S_1^{*PNC}S_{0_\nu}^{PC}\right], \quad (11)$$

where only the S-matrix elements with $l = 0$ are taken into account. Note that the parity-conserving elements S_J^{PC} involve the nonvariable parameters of the s-resonances obtained by analyzing the P-even correlations, whereas the parity-violating elements S_J^{PNC} involve the fitted amplitudes of the fission widths $\Gamma_{f\lambda}^{sp}$ which determine small contributions to the s-resonances from the nearby p-resonances through parity violation. Equation (11) takes into account the existence of two fission channels for the s-resonances with spin $J = 0$.

We write down the S-matrix in terms of the K-matrix in a standard from. To this end, we denote

$$S_{Jnf} \equiv 2e^{-i\phi_n}W_{Jnf},$$

where

$$W_{Jnf} = [(I - K_J)^{-1}]_{nf}. \quad (12)$$

Then, we obtain

$$\frac{1}{4}\mathrm{Im}(S_1^*S_0) = \sin\Delta(\mathrm{Re}\,W_1\,\mathrm{Re}\,W_0 + \mathrm{Im}\,W_1\,\mathrm{Im}\,W_0) + \cos\Delta(\mathrm{Re}\,W_1\,\mathrm{Im}\,W_0 - \mathrm{Im}\,W_1\,\mathrm{Re}\,W_0),$$

where $\Delta = \varphi_s - \varphi_s = 0$, $\sin\Delta = 0$, and $\cos\Delta=1$. As a result, we obtain [9]

$$\sigma^{PNC} = \frac{2\pi}{k^2}\sqrt{3}p_n \times\Bigg[\sum_{\nu}(\mathrm{Re}\,W_1^{PC}\,\mathrm{Im}\,W_{0_\nu}^{PNC} - \mathrm{Im}\,W_1^{PC}\,\mathrm{Re}\,W_{0_\nu}^{PNC}) - \sum_{\nu}(\mathrm{Re}\,W_1^{PNC}\,\mathrm{Im}\,W_{0_\nu}^{PC} - \mathrm{Im}\,W_1^{PNC}\,\mathrm{Re}\,W_{0_\nu}^{PC})\Bigg], \quad (13)$$

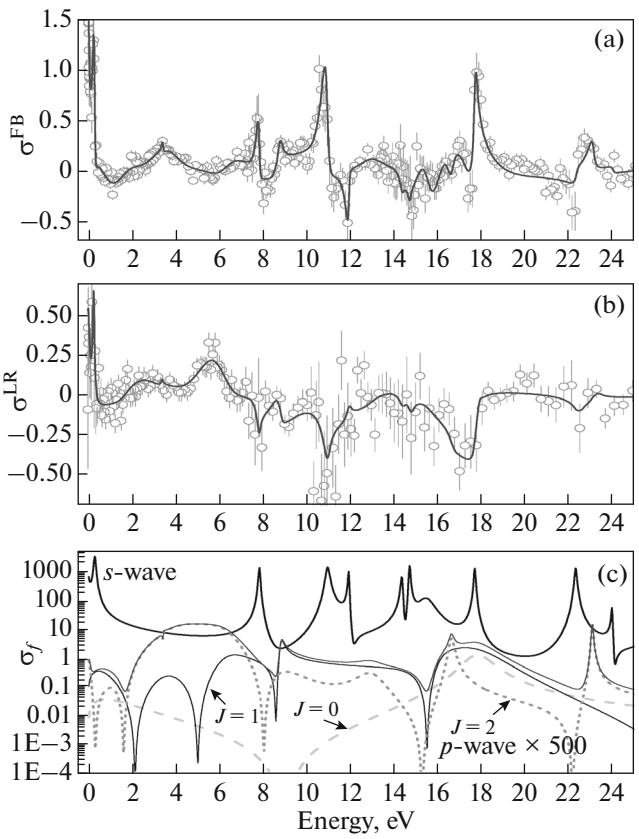

Fig. 5. The fits (solid curves) of the measured cross sections (data points with error bars) $\sigma_{nf}^{FB}(E)$ (top panel b) and $\sigma_{nf}^{LR}(E)$ (medium panel b). Experimental s-wave and calculated p-wave total fission cross sections and the breakdown of the latter to spin components.

and the elements of the K-matrix for the compound states λ with spin J have a form

$$K_{ij} = -\frac{1}{4}\sum_{\lambda}\frac{\Gamma_{\gamma\lambda}\sqrt{\Gamma_{i\lambda}\Gamma_{j\lambda}}}{d_\lambda} + \frac{i}{2} \times \sum_{\lambda}\frac{(E_\lambda - E)\sqrt{\Gamma_{i\lambda}\Gamma_{j\lambda}}}{d_\lambda}, \quad d_\lambda = (E_\lambda - E)^2 + \Gamma_{\gamma\lambda}^2/4. \quad (14)$$

We assume that the admixtures of the s-p fission amplitudes to the s-resonances are related to the fission amplitudes of p-resonances through

$$\gamma_{f\lambda}^{sp} = \sum_{\mu}\frac{\langle p_\mu|H_W|s_\lambda\rangle}{E_\mu - E_\lambda}\gamma_{f\mu}^{p}, \quad (15)$$

where $\langle p_\mu|H|s_\lambda\rangle$ are the matrix elements of the weak neutron—nucleus interaction and $\gamma_{f\lambda}^{sp} = \sqrt{\Gamma_{f\lambda}^{sp}}$.

The results of the analysis [9, 10] of P-even forward—backward and left—right correlations for ^{239}Pu are shown in Fig. 5. When analyzing the P-odd effects,

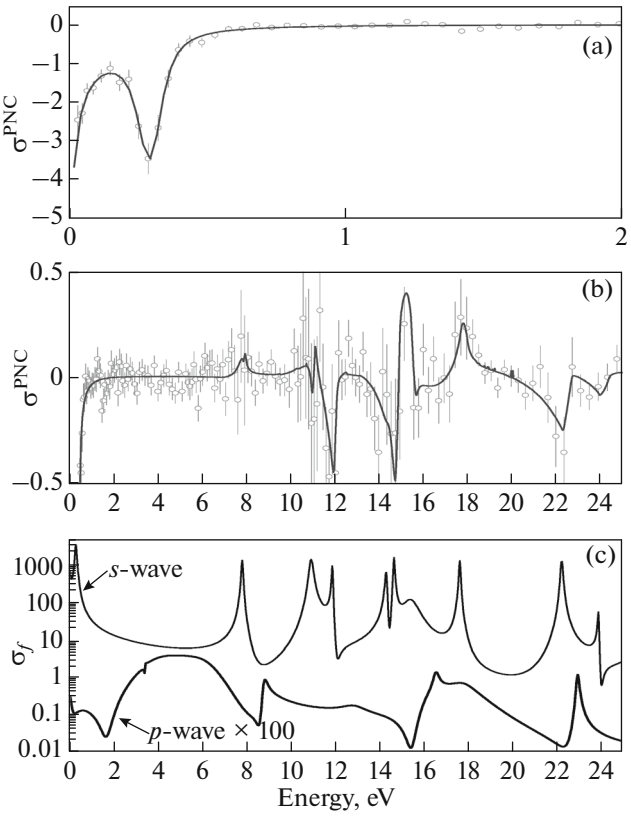

Fig. 6. One of the acceptable fits of measured values ofs) $\sigma_{nf}^{PNC}(E)$ (top p(data points) is shown by solid curves in (a) and (b). Shown in (c) are the *s*- and *p*-wave fission cross sections.

the parameters of the s- and p-resonances were fixed in the fitting procedure. The parameters have been obtained by fitting the cross sections and the *P*-even effects, and only the amplitudes of the mixed-parity widths $\Gamma_{f\lambda}^{sp}$ were varied. One of the fits of the parity-violating *P*-odd effect for ^{239}Pu [9, 10] is shown in Fig. 6.

According to Eq. (15), the amplitude $\gamma_{f\lambda}^{sp}$ is expressed through the matrix element of the weak neutron—nucleus interaction $\langle p_\mu | H | s_\lambda \rangle$ and the fission amplitudes of *p*-wave resonances. Generally speaking, either these matrix elements or the amplitudes $\gamma_{f\mu}^{p}$ can have arbitrary signs. However, as soon as we wish to set a lower limit on the absolute value of $\langle p_\mu | H | s_\lambda \rangle$, positive signs should be assigned to all terms in the sum in Eq. (15). The parameter values returned by the best fit resulted in the lower limit

$$|\langle p_\mu | H | s_\lambda \rangle| \geq 2.4\,\text{meV}.$$

This is consistent with the estimates obtained in other experiments [26] and, in particular, in those that involve transmitting polarized neutrons through the targets of heavy nuclei.

3. INVESTIGATIONS OF *T*-ODD EFFECTS IN FISSION

An experimental search for the *T*-odd three-vector correlation in the ternary fission of ^{233}U induced by cold polarized neutrons was carried out in 1998 by a Russian—German collaboration using the high-flux reactor at the Laue—Langevin Institute [27]. The investigated correlation has the form

$$W = 1 + D_\alpha(\sigma_n \cdot [p_{lf} \times p_\alpha]). \quad (16)$$

Here, D_α is the correlation factor, σ_n is the spin of the neutron captured by the ^{233}U nucleus, and p_α and p_{lf} are the momenta of the α-particle emitted in ternary fission and of the light fragment, respectively. All vectors are normalized.

A similar experiment for testing the time-reversal invariance of nuclear forces was earlier proposed in [28]. The asymmetry in the counting rates of α coincidences with a light and a heavy fragment upon reversing the direction of neutron-beam polarization was measured. The estimated value of the D_α factor proved to be unexpectedly high: on the order of 10^{-3}. However, the existence of this correlation does not unequivocally prove that the time-reversal invariance is violated: in inelastic nuclear reactions, a *T*-odd correlation may arise from the final-state interaction or from the interference of the reaction amplitudes for neighboring compound states.

Therefore, alternative mechanisms for the three-vector correlation had to be revealed. Several models have been proposed for explaining the effect [29–31]. Although in all these models the discussed effect is described without invoking the time-reversal violation, formally it is *T*-odd and is still referred to as the TRI effect.

A detailed investigation of the three-vector correlation using eight spatially separated detectors of α-particles [32] revealed an additional dependence of measured asymmetries on detector positions. The observed anomaly could not be explained by any systematic effects, and the authors concluded that there exists yet another *T*-odd effect arising from the rotation of the fissioning polarized nucleus prior to the breakup. This was called the ROT effect.

The underlying mechanism suggests that due to the rotation of a nucleus polarized perpendicular to the plane defined by the centers of the target and of the detectors of fragments and α-particles, the fragment trajectory being straight for the non-rotating nucleus becomes parabolic. Therefore, for the fragment from a fission event involving the emission of an α-particle to impinge on the detector, the deformation axis of the fissioning nucleus must form a small angle Δθ with the direction towards the detector. The value of this angle depends both on the rotation speed of the nucleus and on the fission mode, because the parameters of the fragment trajectory depend on the ratio between the orbital and linear components of its velocity. The

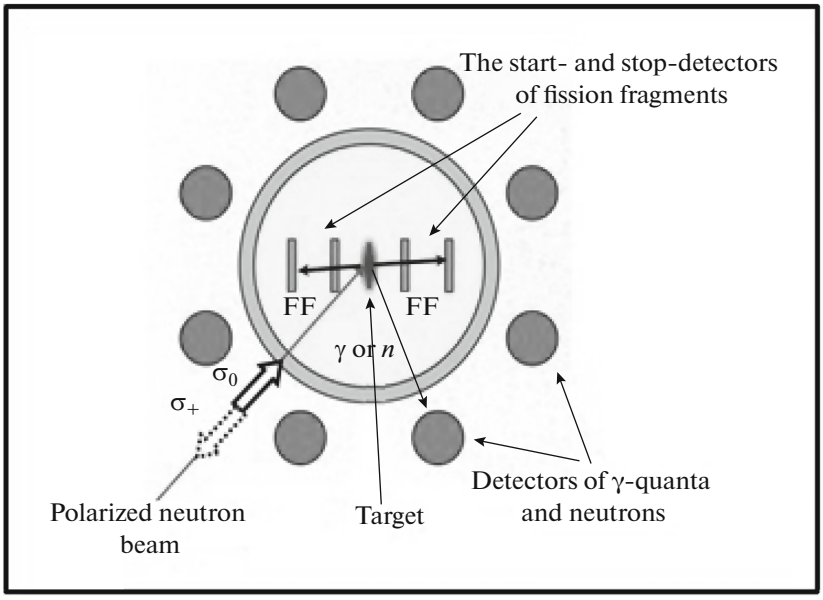

Fig. 7. The layout of the experiments [34–37].

angular distribution of α-particles is formed with respect to the nucleus deformation axis, and therefore will rotate by the same small angle. Upon reversion of the polarization of the neutron beam which induces the fission, the polarization of the compound nucleus changes sign together with the direction of the rotation. Thus, the angle by which the angular distribution of α-particles is shifted also changes its sign. Therefore, the measured effect reflects a relative shift of the α-particle angular distribution by the angle $2\Delta\theta$ upon reversion of the direction of the neutron-beam polarization.

The above quasi-classical description of the ROT effect suggests that the angular distribution of any particle emitted in the fission together with the two fragments may show an analogous phenomenon, provided that this distribution is anisotropic with respect to the deformation axis of the fissioning nucleus at the moment of rupture, and that the anisotropy is fully or partially retained with respect to the original direction of the deformation axis after the fragments separate to infinity. The ROT effect in the emission of prompt γ-quanta and neutrons in binary fission of the ^{235}U and ^{233}U nuclei induced by polarized cold neutrons has been investigated in a series of experiments by the LNP-JINR—ITEP collaboration [33–37].

Most of these experiments employed the MEPHISTO facility of the reactor FRM II at the Technical University of Munich [34–37]. The setup for measuring the *T*-odd effects in nuclear fission is shown in Fig. 7. A longitudinally polarized beam of cold neutrons impinged on a target placed at the center of the fission chamber. The fragments were detected by fast multiwire chambers and classified as light or heavy by time-of-flight technique. Gamma-quanta and neutrons were detected by the plastic and NaI(Tl) scintillation counters placed at different angles with respect to the direction of fragment emission. The measurements referred to the so-called TRI effect (the up—down asymmetry of particle emission) and the ROT effect that consists in an angular shift of the fissioning system in either direction with respect to the angular momentum brought by the polarized neutron.

A series of experiments revealed no TRI-correlation for neutrons beyond the measurement error of 2.3×10^{-5}. An upper limit was set on the asymmetry factor: $|D_n| < 6 \times 10^{-5}$ at 99% C. L. Likewise, no TRI effect was detected for the prompt γ-quanta, for which it is not predicted by any model. The ROT effect was also investigated for both the γ-quanta and neutrons. For the first time, the ROT effects in the γ and neutron emission were found to have opposite sign for the ^{235}U and ^{233}U nuclei. The results of the latter investigation in which the ROT effect was simultaneously measured for these two nuclei are presented in Table 1.

The reported results disagree with the data for the ROT effect in the angular distribution of light charged particles in ternary fission [38, 39] where the signs of the ROT effect were found to be the same for the ^{235}U and ^{233}U nuclei. This disagreement merits further investigation and may indicate that the state-of-the-art model poorly describes the ROT effect in ternary fission.

Table 1. ROT asymmetry in 10^{-5} units

Fission products	Angle to the fission axis, deg	^{233}U	^{235}U
γ-quanta	22.5	$+2.8 \pm 1.7$	-12.9 ± 2.4
γ-quanta	45	$+6.3 \pm 1.6$	-16.6 ± 1.6
γ-quanta	67.5	$+6.8 \pm 2.4$	-20.0 ± 1.8
Neutrons	22.5	$+4.8 \pm 1.6$	-21.2 ± 2.5

In the analysis [40] based on the model approach developed in [14–16], the ROT effect for the γ-quanta emitted in binary fission was formulated as

$$\frac{d\sigma}{d\Omega_\gamma} = \sum_{Q,\Lambda,H} \tau_{Q0}(J) B(Q,\Lambda,H) \Phi^H_{MQ}(n_\gamma, n_{LF}, n_J), \quad (17)$$

where n_γ, n_{LF}, n_J are unit vectors along the γ and light-fragment directions and that of spin polarization, and $\tau_{Q0}(J)$ is the spin-tensor that describes the spin orientation of the fissioning nucleus. We have $\tau_{00}(J) = 1$ and $\tau_{10}(J) = p(J)\sqrt{J/(J+1)}$, where $p(J)$ is the compound-nucleus polarization upon the polarized-neutron capture by the target nucleus. The reaction dynamics is determined by the factor $B(Q,\Lambda,H)$, which comprises bilinear combinations of fission amplitudes involving the emission of two fragments. The term in (17) corresponding to $Q = 1$ and $\Lambda = H = 2$ describes the five-vector T-odd angular correlation

$$\Phi^2_{21}(n_\gamma, n_{LF}, n_J) \sim (n_\gamma [n_J \times n_{LF}](n_\gamma n_{LF}), \quad (18)$$

which determines the ROT effect.

Quite nontrivially, the factor $B(Q,\Lambda,H)$ includes the product of three Klebsch–Gordan coefficients $C^{Qh}_{Hh\Lambda 0} C^{JK'}_{JKQh} C^{FF}_{FKHh}$, where F and F' are the total spins in the exit fission channel, and K and K' are their projections to the fragments emission axis n_J. One might presume that the interference terms with $K \neq K'$ should vanish upon summing over all binary channels. However, the equality $K = K'$ implies $h = 0$, and then we have $C^{Q0}_{H0\Lambda 0} = 0$ for $Q = 1$, $\Lambda = H = 2$. Therefore, the experimental observation of a small ($\sim 10^{-4}$) 5-vector angular correlation proves that some mixing in K occurs in exit channels of nuclear fission. This quantifies the violation of the helicity quantum number $\tilde{K}$ at the rupture point of the fissioning nucleus caused by a small (but nonvanishing) centrifugal barrier for the fission fragments. This also allows estimating the accuracy of the approximate relation $K \approx \tilde{K}$ between the projection K of the fissioning-nucleus spin J and the helicity quantum number that characterizes the effective fission channel $J^\pi \tilde{K}$. We can conclude that Bohr's scheme of effective fission channels is validated by the formalism [14–16] based on the helicity representation pioneered by Strutinskii [17].

Note that by measuring the ROT effect for isolated neutron resonances, one can estimate the distribution of weights for different K values in these compound states. However, such measurements pose challenging experimental problems.

The following conclusions concerning fundamental properties of nuclear fission induced by the resonance and thermal neutrons may be drawn from the aforementioned experimental and theoretical results (see [40, 41] for further details).

(1) The measured total and differential cross sections of the fission reaction reveal the interference between different resonances, which reflects the quantum-mechanical nature of nuclear fission. As consistently demonstrated by the theoretical analyses [14, 19], the phase space of binary channels of the fission fragments c_f with dimension $\sim 10^9$ may be reduced to the space of a limited number of "effective" channels $J^\pi K$ upon summation over different fragment states, which is realized in any experiment. The exit channel of binary fission c_f is described by the spin of the fissioning system J with projection M to the z-axis, the total spin of the channel $\mathbf{F} = \mathbf{J}_1 + \mathbf{J}_2$ with projection $\tilde{K}$ to the fragment-emission axis, the channel parity Π, and the quantum numbers of fragments including their parities π_1 and π_2. In the helicity representation for the wave function $\tilde{\Psi}^{F\tilde{K}\Pi JM}_{c_f}(\Omega_{n_f}, \{\varphi_1^{J_1\pi_1}(\chi_1)\varphi_2^{J_2\pi_2}(\chi_2)\}^{c_f}_{F\tilde{K}})$ of the exit channel c_f, the differential cross section of the (n,f) reaction is written as follows [16, 41]:

$$\frac{d\sigma^{c_f}}{d\Omega_f} = \pi\hat{\lambda}^2 \sum_{J'J} (g_{J'} g_J)^{1/2} \times \sum_{l'j'lj} \sum_Q \Phi^Q_{l'j'ljJ'J}(\mathbf{n_f n_k n_I n_s}) B^{c_f}_Q(l'j'lj; J'J), \quad (19)$$

where l and j are the orbital momentum and total spin of the entrance neutron channel. The kinematic factor Φ^Q depends only on the relative orientation of the unit vectors $\mathbf{n_k}$, $\mathbf{n_s}$, $\mathbf{n_I}$, ans $\mathbf{n_f}$, which is determined by the experimental conditions, where $\mathbf{n_k}$ is directed along the collision axis in the entrance channel and $\mathbf{n_s}$ and $\mathbf{n_I}$ follow the orientations of the neutron spin s and of the target-nucleus spin I, respectively. The factor $B^{c_f}_Q$ fully describes the reaction dynamics which is determined by the bilinear combinations of the S-matrix elements $S(l, j \to F\tilde{K}\Pi c_f)$. However, the differential cross section (19) is virtually unobservable: the channels c_f of the primary fragments prior to emission of prompt fission neutrons, which are strongly deformed and relatively cold, are summed over in a realistic experiment. Retained in the sum are the interference terms in the differential cross section that determine the observable angular correlations of fission fragments. This is due to

the structure and symmetry properties of the transitional-state wave function of a general form $\Psi_f^{J\pi KM}(\Omega_f, \{\chi\},\{\beta\})$ as suggested by the collective model of the nucleus, where $J^\pi KM$ are the aforementioned quantum numbers and $\{\beta\}$ are the parameters that determine the position of the fissioning system in the configuration space of deformations. This wave function describes the possible "motion trajectories" of the fissioning nucleus in the configuration space until the breakup into fragments. It carries the shell structure of the fissioning nucleus, which determines the discrete set of possible prefission configurations (or fission modes), as well as the major characteristics of corresponding fission barriers. The amplitude of the function $\Psi_f^{J\pi KM}(\Omega_f, \{\chi\},\{\beta\})$ for $\{\beta\} = \{\beta\}_{\text{ground}}$, which corresponds to the compound-nucleus deformation upon the neutron capture, is determined by the weight $a_\lambda^{J\pi K}$ of the component with the given value of K in the wave function

$$X_\lambda^{J\pi M}(\{\chi\}) = \sum_K a_\lambda^{J\pi K}\Phi_\lambda^{J\pi KM}(\{\chi\}) \qquad (20)$$

of the neutron resonance λ. The highly excited compound state is described by an extremely complex wave function (20), in which the components with different spin projections K are strongly mixed by the Coriolis interaction, as discussed in Section 2 above. Therefore, the distribution of the weights $a_\lambda^{J\pi K}$ of its components $\Phi_\lambda^{J\pi KM}(\{\chi\})$ for a given resonance λ is statistical and should strongly vary from resonance to resonance, as indeed demonstrated by the data of Fig. 3. This causes a strong variation of fission widths, first considered by Porter and Thomas [42] using a simplified version of the statistical model.

Within the standard R-matrix parametrization, the S-matrix elements $S(l, j \to F\tilde{K}\,\Pi c_f)$ depend on the fission-width amplitudes $\gamma_{\lambda f}^{JF\tilde{K}\Pi c_f}$. These are determined by sewing together the wave function of the transitional state $\Psi_f^{J\pi KM}(\Omega_f, \{\chi\},\{\beta\})$ and that of the fission channel c_f, $\tilde{\Psi}_{c_f}^{F\tilde{K}\Pi JM}(\Omega_{n_f}, \{\varphi_1^{J_1\pi_1}(\chi_1)\varphi_2^{J_2\pi_2}(\chi_2)\}_{F\tilde{K}}^{c_f})$. This leads to the conditions $K = \tilde{K}$, $\Pi = \pi$, and allows us to derive the expressions for the amplitudes $\gamma_{\lambda f}^{JF\tilde{K}\Pi c_f}$ which, in their turn, allow to carry out the summation in (19) over all exit channels c_f required by the particular experimental conditions. The resultant "observable" differential cross section retains the previous structure, but the factor $B_Q^{c_f}$ is now expressed through the elements of the reduced multilevel S-matrix $S_J(l, j \to K\pi f)$defined for the effective channel $J^\pi K$. The reduced S-matrix includes the fission amplitudes of neutron resonances summed over the fragment states $\gamma_{\lambda f}^{J\pi K}$, which are proportional to the quantities $a_\lambda^{J\pi K}$. As discussed above, the latter explains the strong variation of partial fission widths.

(2) Phenomenologically, the experimental investigation of P-even and P-odd angular correlations of the fragments suggests that the fission process is nearly adiabatic, *i.e.,* the internal wave function of the fissioning nucleus that carries the quantum number K is defined at each point of the motion trajectory in the deformation space. The orientations of the spin and deformation axis of the fissioning nucleus are described by the collective part of the transitional-state wave function $\Psi_f^{J\pi KM}(\Omega_f, \{\chi\},\{\beta\})$. The fact that the aforementioned correlations are retained upon the experimental "summation" over the multiple binary channels places definite restrictions on the symmetry properties of the function $\Psi_f^{J\pi KM}(\Omega_f, \{\chi\},\{\beta\})$ and, correspondingly, on the characteristics of the two-humped fission barrier. In particular, the modes of asymmetric fission imply the breakup of a pear-shaped nucleus. Consequently, the fission barriers are described by the quantum numbers $J^\pi K$ and, for $K = 0$, by the signatures s and r. Obviously, the fissioning nucleus preserves axial symmetry throughout its path in the deformation space until the breakup.

(3) According to the well-known arguments of the classical liquid-drop model for nuclear fission [43], the nucleus may break up to fragments only upon a strong deformation of the fissioning system. However, this model fails to account for the asymmetric fission. The multimode fission, including the asymmetric one, is a manifestation of the shell structure of the fissioning nucleus [44, 45]. As shown in [46] within the shell-model framework, the breakup of a heavy deformed nucleus to two fragments is strongly suppressed for small deformations by the vanishingly small probabilities for preformation of the latent fragments. The fission process becomes observable only as soon as these probabilities reach some 10^{-6}–10^{-3} with increasing deformation of the system. The deformation of the nucleus brings about changes in its shell structure which, in their turn, give rise to bifurcations of the trajectory in the deformation space that lead to various fission modes. In this scheme, the characteristics of the second deformation barrier depend on the mode m. Therefore, rather than invoke the so-called "transitional states in the saddle point" [43], we consider a set of two-humped fission barriers with quantum numbers J, π, K, s, and r for all accessible fission modes.

The ratio between the total widths of the ternary and binary fission is known to be virtually the same for all neutron resonances [47]. This implies that the breakup of a nucleus into two and three fragments occurs from the same prefission states whose probabilities are determined by the values of barrier parameters for each fission mode.

(4) The discussion in item 1 above implies that the angular distribution of the products of the reaction (n,f), both for the primary channels c_f of binary fission and for the experimentally observable final states, are formed at the breakup point of the fissioning nucleus and are not affected by the subsequent (probably nonadiabatic) transformation of primary fragments that results in their excitation. The internal wave functions of the detected fission fragments differ from those of primary fragments at the breakup point, since the deformation of the fragments is reduced with time and they emit neutrons and γ-quanta. However, the experiment and the theoretical analysis suggest that the coherence of partial amplitudes of the binary fission channels c_f and the observable angular correlations are not strongly affected by these changes of the fragments wave functions.

(5) The mechanism of the transformation of fragment states upon the emission is still an unsolved problem that needs further investigation. In particular, little is known about the process of fast acceleration of the fragments by strong Coulomb repulsion, which, according to the studies of TRI and ROT effects, strongly restricts the allowed range of fragments orbital momenta. Still, the investigations of nuclear fission induced by resonance and thermal neutrons continue to provide important data on the basic properties of the fission process.

4. INVESTIGATIONS OF THE TERNARY AND QUATERNARY SPONTANEOUS FISSION OF ^{252}Cf

The ternary and quaternary spontaneous fission of ^{252}Cf has been investigated at the Laboratory of Neutron Physics for several years in collaboration with the Prague Technical University using the TimePix detectors [48]. The particles emitted in ternary fission were identified using the ΔE–E technique that allows for discrimination of light charged particles by charge. A 12-μm-thick Silicon counter and a pixel TimePix detector [49] with a 300-μm-thick sensitive layer and pixels of 50 × 50 μm were used as ΔE and E detectors, respectively. The ^{252}Cf source of spontaneous fission and two assemblies of the ΔE–E detectors were placed in a vacuum chamber. The fission fragments and 6.2 MeV α-particles from the spontaneous α-decay of californium were fully absorbed by a 31-μm-thick aluminum foil placed between the source and detectors. Therefore, only the long-range light charged particles emitted in ternary fission could be registered in the detectors.

The particles detected in the experiment ranged from hydrogen to beryllium. For the particles of each type, the energy spectra were plotted and corrected for energy losses in the aluminum foil and in the ΔE detector using the computer code SRIM. The energy spectra of α-particles and lithium and beryllium nuclei (without isotope separation) were obtained for the spontaneous ternary fission of ^{252}Cf. Each energy spectrum was fitted to a Gaussian distribution. The estimated total yields of light charged particles agree with the published data.

The search for a very rare process—a quaternary fission in which two light charged particles are emitted along with the two main fragments—was also carried out in the experiment. This process occurs with an extremely small probability that amounts to some 10^{-6}–10^{-7} of that for the ordinary binary fission. As a rule, the quaternary fission involves the formation of two α-particles which can be emitted independently (the authentic quaternary fission) or can result from the decay of an unstable ^{8}Be nucleus emitted as a third particle (the pseudo-quaternary fission).

As many as 72 events were observed in which two particles were simultaneously detected in one or two telescopes. The energy distribution between the two particles was symmetric for 63 events and asymmetric for 9 events. The former (latter) group was assumed to refer to the α–α (α–t) quaternary fission (see Fig. 8a).

The high position resolution of pixel detectors allowed detection of the events in which the two α-particles are emitted at an extremely small angle to each other. Such events were assumed to arise from pseudo-quaternary fission mediated by the decay of an unstable short-lived ^{8}Be nucleus. The energy spectrum of the emitted ^{8}Be nuclei, reconstructed using the measured α-particle energies, is shown in Fig. 8b. The measured probabilities of the authentic and pseudo- quaternary fission are consistent with previous experimental and theoretical estimates.

5. THE INVESTIGATIONS OF PROMPT FISSION NEUTRONS AND MASS—ENERGY DISTRIBUTIONS OF FRAGMENTS IN NUCLEAR FISSION INDUCED BY RESONANCE NEUTRONS

The spontaneous fission and that induced by thermal and resonance neutrons are classical examples of low-energy fission that occurs at zero excitation energy or that comparable to the height of the fission barrier. In the quasi-classical approximation, nuclear fission is caused by a collective motion of constituent nucleons, which may be viewed as a surface deformation of a liquid nuclear drop formed by nucleons interacting through the Coulomb and nuclear forces. Strutinskii's shell correction [44] to the classical liquid-drop fission model [43] allowed formulating an efficient computational model of the multimodal (MM) fission; see the review paper [45] and references therein. In one of the most popular versions of the lat-

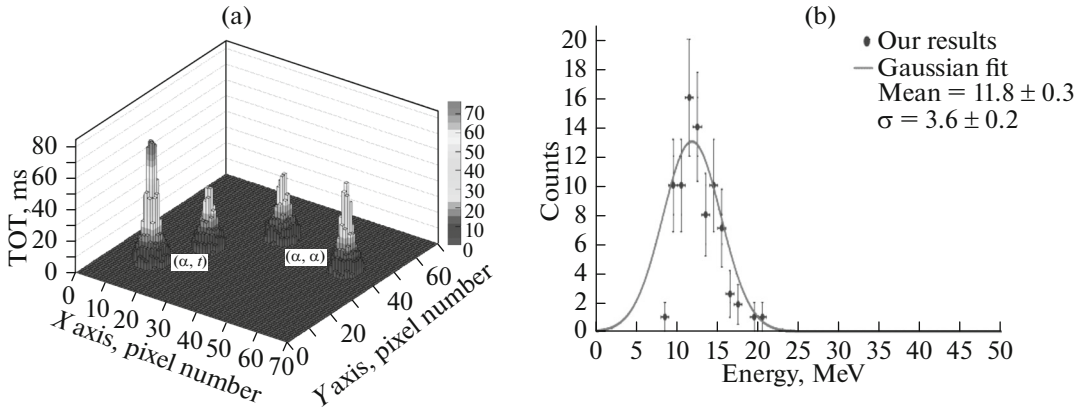

Fig. 8. The examples of clusters for the α–α and α–*t* coincidences (a) and the reconstructed energy spectrum for ^{8}Be (b).

ter model, the shape of the fissioning nucleus affected by growing deformation prior to breakup is represented by quasi-spheroids linked by a sufficiently thick neck. The motion trajectories in the multidimensional deformation space are selected by minimizing the deformation energy of the fissioning system, as estimated according to [44]. As a result, the motion trajectory passes through the valley bottoms of a complex deformation pattern. In the process, the symmetry of the fissile-system shape spontaneously changes at the bifurcation points of the trajectory because the nuclear shell structure changes with increasing deformation. Thus, the fissioning nucleus approaches the region of neck rupture passing through the first (symmetric) barrier and second barriers with symmetric and asymmetric system shape along the trajectories of different length. These trajectories form a discrete set of possible prefission configurations that determine the properties of fission modes (FM). The hypothesis of random neck rupture (RNR) allows one to form the mass distribution (MD) of fission fragments (FF) as a superposition of those for different FMs. The rupture of the neck is followed by the emission of FFs that are accelerated by powerful Coulomb repulsion. As a result, the FFs acquire significant kinetic energy, which may reach ~ 200 MeV on total. The primary FFs formed upon the neck rupture are relatively "cold" and strongly deformed. Upon the emission, the fragments' deformation energy is assumed to transform to that of excitation. Thereupon, prompt fission neutrons (PFN) may be emitted by the excited and fully accelerated FFs.

The number $\bar{\nu}(A,TKE)$ of PFNs emitted by an FF with mass number A and total kinetic energy (TKE) equal to TKE is directly related to the FF excitation spectrum. Measuring the function $\bar{\nu}(A,TKE)$ allows us to obtain the PFN characteristics averaged over A or TKE by integration over the corresponding variable if the mass—energy distribution (MED) of the FF, $Y(A, TKE)$, is known. The examples of such averaging and the MED normalization are shown below:

$$\bar{\nu}(A) = \frac{\int_0^\infty \bar{\nu}(A,TKE)Y(A,TKE)dTKE}{\int_0^\infty Y(A,TKE)dTKE},$$

$$\bar{\nu} = \int_0^\infty \bar{\nu}(A,TKE)Y(A,TKE)dTKEdA, \qquad (21)$$

$$200 = \int_0^\infty Y(A,TKE)dTKEdA.$$

In the models of multimode fission referred to as MM–RNR [45], the FF mass distribution results from the random neck rupture for different prefission configurations. Each of the latter configurations i is realized with a definite probability p_i , so that

$$\sum_{i=1}^{N} p_i = 1, \qquad (22)$$

where N is the number of possible FMs. Each FM i involves a mass distribution $Y_i(A)$ normalized according to

$$\sum_{A=0}^{A_{CN}} Y_i(A) = 2 \qquad (23)$$

and a PFN multiplicity $\bar{\nu}_i(A)$ which depends on A. The primary (prior to PFN emission) mass distribution $Y(A)$ is formed as a sum over all accessible FMs,

$$Y_i(A) = \sum_{A=0}^{A_{CN}} p_i Y_i(A), \qquad (24)$$

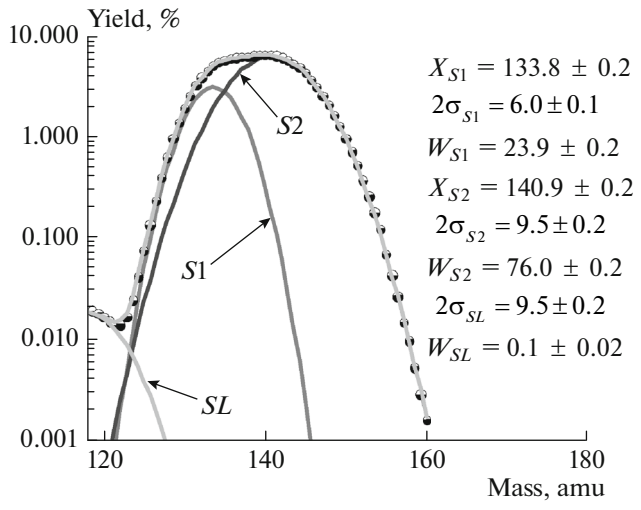

Fig. 9. Decomposition of the mass distribution of the fragments of ^{235}U fission induced by thermal neutrons into different fission modes, as computed using the MM-RNR model.

as illustrated in Fig. 9. Thus, the experimentally measured PFN multiplicity is a superposition of the $\bar{\nu}_i(A)$ distributions for different FMs:

$$\bar{\nu}(A) = \frac{\sum_{i}^{N} p_i Y_i(A)\bar{\nu}_i(A)}{\sum_{A=0}^{A_{CN}} p_i Y_i(A)}. \quad (25)$$

The analysis of experimental data on PFNs allows one to obtain the relation [49]

$$\bar{\nu}(A,TKE) = \left\{\frac{\partial\bar{\nu}}{\partial TKE}(A)[TKE_{\max} - TKE(A)], \text{ if } TKE < TKE_{\max}\right\}. \quad (26)$$

The experimental data also suggest that for the given mass number A the function $\bar{\nu}(A,TKE)$ is linear in TKE, so that $\bar{\nu}(A,TKE)$ can be obtained by measuring the functions $\bar{\nu}(A)$ and $TKE(A)$. Combining equations (21) and (26), we obtain

$$\bar{\nu}(A) = \int_0^\infty \bar{\nu}(A,TKE)Y(A,TKE)dTKE = \frac{\partial\bar{\nu}}{\partial TKE}(A)\left[\int_0^{TKE_{\max}(A)} TKE \cdot Y(A,TKE)dTKE - TKE_{\max}(A)\int_0^{TKE_{\max}(A)} Y(A,TKE)dTKE\right]. \quad (27)$$

The dependences of the mean number of PFNs on the FF mass and total kinetic energy are shown in Fig. 10. The saw-like shape of the function $\bar{\nu}(A)$ directly proves that the neck rupture of the fissioning system is a random process. The large tangent of the saw inclination angle to the mass axis finds an explanation in the framework of the MM–RNR model [45].

The quantum properties of the fission process can best be revealed in investigations of the (n,f) reaction induced by resonance neutrons, as discussed in detail in Sections 2 and 3 above. However, the variables discussed there were averaged over the masses and energies of the fragments. The variation of total kinetic energy in the resonances of the ^{235}U(n,f) reaction was investigated in [53–56]. The results of these measurements are shown in Fig. 11. The spread of the fluctuations is seen to be within 0.1% of the mean value of total kinetic energy. In the right panel of Fig. 11, the observed mass distribution of fission fragments is reproduced by the MM-RNR prediction taking into account the asymmetric fission modes "standard1" (S1) and "standard2" (S2) and the symmetric mode "superlong" (SL).

The aforementioned experimental results can be interpreted by combining the theoretical approaches

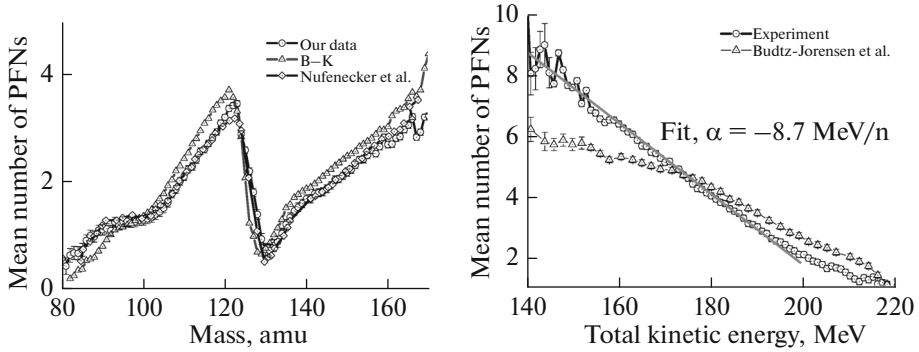

Fig. 10. The mean number of prompt fission neutrons (PFNs) as a function of the mass (left panel) and total kinetic energy (right panel) of fission fragments, as measured in [51] and [52].

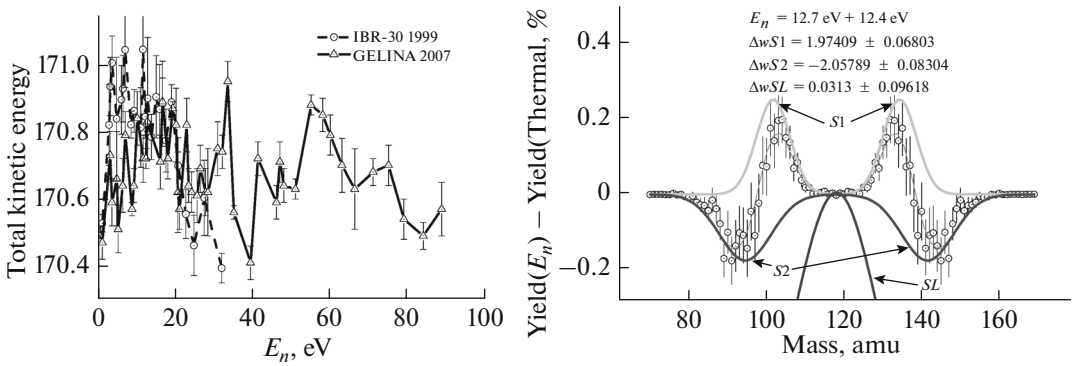

Fig. 11. The fluctuation of the total kinetic energy of fission fragments as a function of resonant-neutron energy measured with the IBR-30 and GELINA neutron sources (left panel), and the mass distribution of fission fragments in the vicinity of the resonance with E_n =12.5 eV (right panel).

developed in [16] and [45]. Following [16], TKE of fission fragments in the resonance λ with spin—parity of J^π is expressed as

$$E_\lambda^{J\pi} = \sum_K \omega_\lambda^{J\pi K} \sum_i p_i^K E_i^K = \sum_K \omega_\lambda^{J\pi K} E^K, \qquad (28)$$

where $\omega_\lambda^{J\pi K}$ are the weights of the components with the given value of K in the compound state λ normalized according to $\sum_K \omega_\lambda^{J\pi K} = 1$, and p_i^K are the probabilities for realizing the fission modes i first introduced in [20]. (Note that in contrast with the probabilities p_i in Eq. (22), these depend on the projection K.) The TKE of the fragments for the mode i are determined as follows:

$$E_i^K = \frac{\int E Y_i^K(A,E)\,dE\,dA}{\int Y_i^K(A,E)\,dE\,dA} \qquad (29)$$

and E^K denotes the TKE for the given K summed over all accessible fission modes. Then, the TKE fluctuation with respect to the mean value

$$\langle E^{J\pi} \rangle = \sum_\lambda^N E_\lambda^{J\pi} / N = \sum_K E^K \langle \omega^{J\pi K} \rangle \qquad (30)$$

acquires a form

$$\Delta E_\lambda^{J\pi} = \sum_K E^K \Delta\omega_\lambda^{J\pi K}, \qquad (31)$$

where $\Delta\omega_\lambda^{J\pi K} = \left(\omega_\lambda^{J\pi K} - \langle \omega^{J\pi K} \rangle\right)$ is the weight variation for the component with the given K in the resonance λ. The fluctuations $\Delta E_\lambda^{J\pi}$ are small as soon as the energy E^K weakly depends on K $(E^K \approx \bar{E})$, because for this case we have

$$\Delta E_\lambda^{J\pi} \approx \bar{E}\left(\sum_K \omega_\lambda^{J\pi K} - \sum_K \langle \omega^{J\pi K} \rangle\right) \ll 1 \qquad (32)$$

taking into account the normalization of the weights $\omega_\lambda^{J\pi K}$.

Therefore, small (~10^{-3}) fluctuations $\Delta E_\lambda^{J\pi}$ measured in [53–56] definitely indicate that the FF kinetic energy E^K summed over all FMs weakly depends on K. This explains the predictive accuracy of the quasi-classical MM-RNR model [45] in which the weights p_i are independent of the projection K, see equation (22). In some sense, the smallness of the fluctuations $\Delta E_\lambda^{J\pi}$ reflects the quasi-classical character of the integral characteristics like the TKE and the mass—energy distribution, whereas the quantum-mechanical characteristics of the fission process like the weights $\omega_\lambda^{J\pi K}$ and partial fission widths are subject to strong fluctuations due to a complex structure of compound states.

6. DEVELOPMENT OF THE METHODS FOR INVESTIGATING THE CHARACTERISTICS OF NUCLEAR FISSION

The evolution of technology has dictated a transition from the analogue to digital signal processing (DSP) in nuclear electronics [57–61]. In DSP, the analogue detector signal is transformed to a sequence of voltage values measured at regular time intervals. As soon as the signal is discretized in agreement with certain rules [62], the complete information of the original analogue signal is transferred to its digital image. The digitized detector signals that refer to selected events may be logged and stored throughout the experiment. The logged events may be fully and multiply reproduced in the detected form. This implies a qualitatively new level of experimental investigations. In such experimental arrangement, a key role belongs to the program software (PS) whereby DSP is realized. A number of DSP algorithms that refer to FF spectroscopy and PFN emission in low-energy nuclear fission

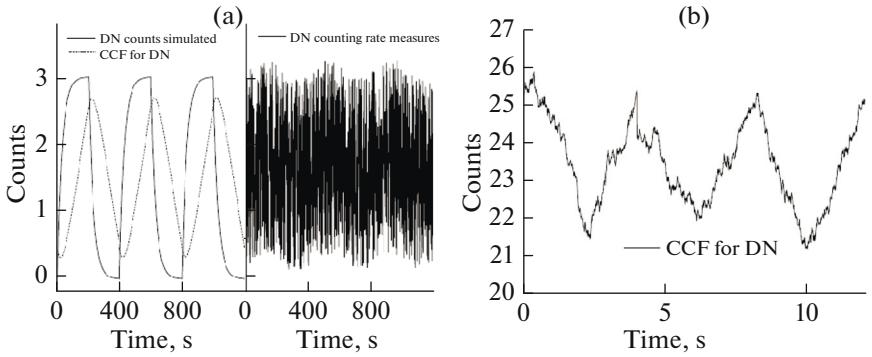

Fig. 12. The simulated and measured mutual correlation functions between the yield of delayed neutrons and the meander-modulated flux of thermal neutrons (a) and the measured mutual correlation function after ~200-fold averaging (b).

have been developed at LNP JINR over the last two decades.

In one of the initial applications, DSP was employed for analyzing the correlations in the investigation of the yield of delayed neutrons in the fission of ^{237}Np nuclei induced by thermal neutrons [63]. The data of Fig. 12 demonstrate that after relatively small number of averaging the measured correlation function approaches the simulated one. This method has allowed to measure the yield of delayed neutrons from the reaction ^{237}Np(n, f) despite a very low signal-to-background ratio.

The current investigations of nuclear fission at low excitation energies are based on the experimental techniques, the equipment for detecting the fission fragments in correlation with PFNs and other fission products, and the methods for data processing and data analysis that have been developed at LNP over the last years. Our future investigations of nuclear fission will rely on the resonance-neutron source IREN expected to start operation at full intensity in the beginning of 2016. At present, the new equipment is being tested in the 11B beam of thermal neutrons from the IBR-2M reactor. Our major task is to construct the apparatus for investigating the emission of prompt neutrons by the fragments of nuclear fission induced by resonance neutrons. To this end, one has to detect PFNs in coincidence with FFs and simultaneously measure the FF masses, the FF and PFN kinetic energies, and the angle between the PFN direction of motion and the fission axis. The previous similar experiments such as [52] employed a classical twin ionization chamber (TIC) with Frisch grids [52, 64]. Unfortunately, in such experimental arrangement no more than two neutron detectors can be deployed because of geometric restrictions imposed by measuring the angle between the PFN direction and the fission axis. This implies a PFN detection efficiency of no more than 0.005 and virtually rules out any investigation of nuclear fission induced by fast and resonant neutrons.

In order to circumvent the aforementioned restriction, we have proposed the experimental scheme with a position-sensitive twin ionization chamber (PS TIC) [65]. Apart from measuring the fragment masses and the PFN and FF kinetic energies, this chamber allows to determine the relative orientation of the fission axis of correlated FFs and PFN direction of motion in the spherical coordinates (θ, φ), as illustrated in Fig. 13. In this arrangement, the PFN detection efficiency can be enhanced to an acceptable level by deploying more neutron detectors, which will provide the projected accuracy in future experiments. Shown in Fig. 13 are the results of the measurements with PS TIC for fixed ranges of $\cos(\theta)$. The angle φ is seen to be uniformly distributed over the circle $R^*\cos(\theta)d\theta$.

To conclude, new fundamental data on the dynamics of the fission process will be obtained from the analysis of experimental data, which can be collected by simultaneously measuring the kinetic energies and the total number of PFNs and the masses and kinetic energies of correlated FFs at low excitation energy of the fissioning nucleus.

7. INVESTIGATION OF DELAYED NEUTRON EMISSION IN THE ACTINIDE FISSION INDUCED BY THERMAL NEUTRONS

The emission of delayed neutrons (DNs) in the neutron-induced fission of actinides is of fundamental importance for realizing a controlled chain fission reaction [66–68]. The yields and time characteristics of DNs in the neutron-induced fission of major and minor reactor isotopes are important nuclear constants used in simulating the kinetics of nuclear reactors. As soon as these constants for many transuranium elements are known, we are able to reach a better understanding of the fission process, as well as to develop the fission models and predict the DN properties for the unexplored nuclei. However, the data on DN emission for the major and most minor actinides are not sufficiently accurate for reliably simulating the nuclear-reactor kinetics for high degrees of fuel burnout in particular, which is essential for nuclear secu-

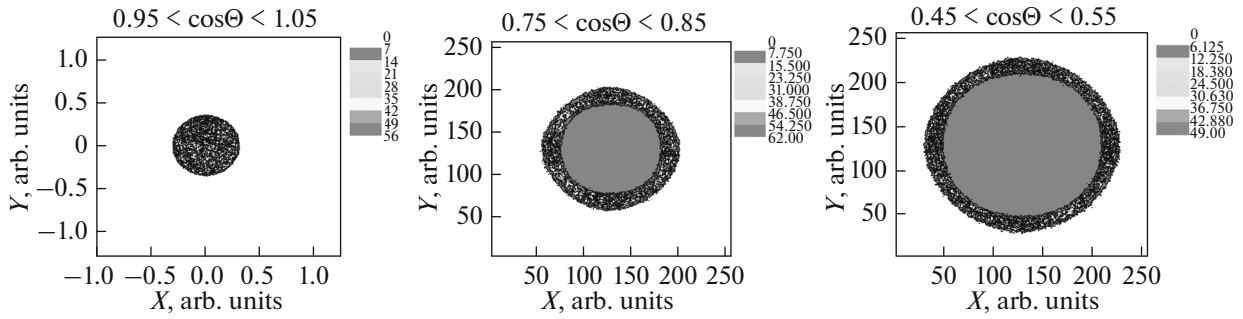

Fig. 13. The distributions of the "centers of gravity" of fission fragments on the (*X*, *Y*) plane formed by the anodes of the position-sensitive TIC for different values of the angle Θ between the fission axis and the applicate axis *Z*.

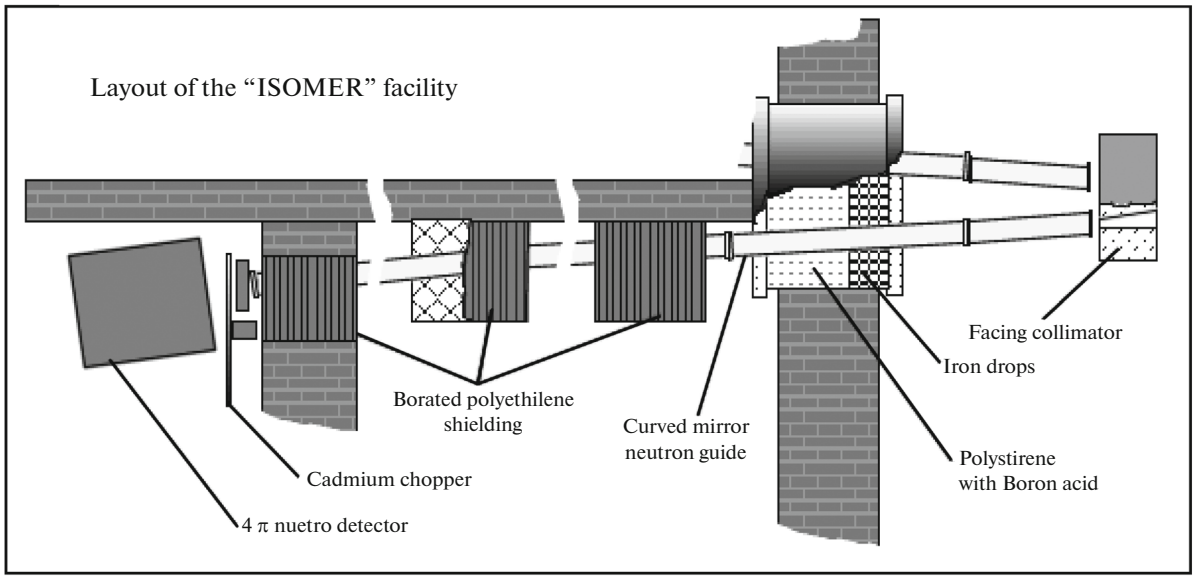

Fig. 14. The schematic layout of the "Isomer" facility operating in the 11B channel of the IBR-2 neutron source.

rity. Therefore, the DN characteristics should be measured to better precision and the existing data should be verified by independent measurements. Apart from that, such measurements allow to test and improve computational methods and phenomenological procedures for extrapolating the DN characteristics to the yet-unexplored isotopes and for estimating the reliability of the available data. In fact, the experimental data often disagree with the calculus for the same isotope.

In order to measure the DN yield in the fission of actinide nuclei induced by thermal neutrons, the "Isomer" facility irradiated by neutrons from the IBR-2 reactor was constructed by LNP JINR in 1993–1995. The experimental method consisted in periodically irradiating a sample with a pulsed neutron beam and measuring the DN yield in time intervals between the pulses [69]. The scheme of the "Isomer" setup is shown in Fig. 14. In the initial experiments with this facility, the DN yields in the fission of the ^{233}U, ^{237}Np, and ^{239}Pu isotopes induced by thermal neutrons were measured [70]. The parameters of the facility were significantly improved by an upgrade in 2004 aimed at perfecting the method and extending a set of investigated nuclei. The upgrade allowed including the neptunium and curium isotopes ^{237}Np and ^{245}Cm in the measurements. The published experimental data had been substantial for the former but insufficient for the latter.

The DN characteristics in the ^{245}Cm fission induced by thermal neutrons with a reactor spectrum were for the first time measured in [71]. The measured value of the absolute total DN yield, ν_d = (0.59 ± 0.04)%, proved to be inconsistent with the estimate ν_d = 0.75% obtained in the same paper by the method of summation over the precursor isomers. The substantially lower ν_d estimates later derived in [72, 73] using the same computational method were consistent

Table 2. The characteristics of the curium sample employed

Isotope	$T_{1/2}$ (α)	Content		Spontaneous fission rate per s	Number of prompt neutrons per event of spontaneous fission	Prompt neutron rate per s
		%	mg			
^{244}Cm	18.1 yr	3.78	0.076	319	2.72	868
^{245}Cm	8500 yr	95.46	1.91	7.8×10^{-2}	≈3	≈0.3
^{246}Cm	4700 yr	0.71	0.014	43	2.95	127

with the experimental ν_d value obtained in [71] within the combined errors. Therefore, an independent ν_d measurement was needed.

The characteristics of the curium sample employed in the experiments with the "Isomer-M" facility are listed in Table 2. Despite a rather high enrichment of the sample with the ^{245}Cm isotope and the large cross section of its fission induced by thermal neutrons (≈2145b), the admixtures of the ^{244}Cm and ^{246}Cm isotopes are seen to generate a constant background of prompt neutrons from spontaneous fission that significantly exceeds the DN counting rate for the investigated isotope ^{245}Cm. By placing the sample inside the ionization fission chamber, we were able to suppress this background by detecting the neutrons in anticoincidence with the fission-fragment signals from the chamber.

Shown in Fig. 15 is the schematic layout of the "Isomer-M" detector module with a target inside the ionization chamber. The method for analyzing the apparatus time spectra obtained in the experiment, shown in Fig. 16, had been developed during the measurements with the ^{237}Np isotope and is detailed in [74]. The total yield of delayed neutrons in the ^{245}Cm fission induced by thermal neutrons was measured as $\nu_d = 0.0064 \pm 0.0002$ [75]. It is consistent with the previous measurement $\nu_d = 0.0059 \pm 0.0004$ [71] and it has a better accuracy.

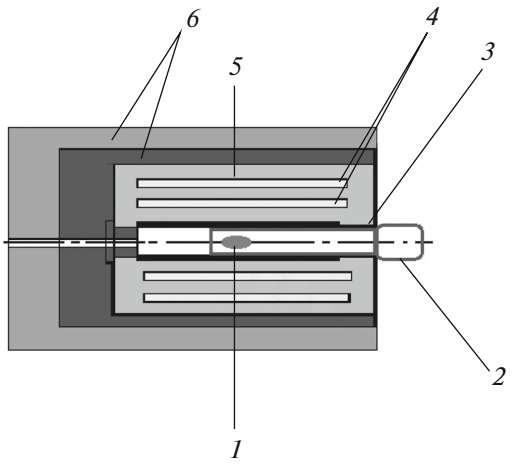

Fig. 15. The schematic view of the detector module of the "Isomer-M" facility showing the ^{245}Cm target (*1*), the ionization chamber filled with the CH_4 gas (*2*), the Cd screen (*3*), the ^{3}He counters (*4*), the moderator of neutrons (*5*), and a combined shielding with CH and CH–B (*6*).

In Fig. 17, the obtained result [75] is added to the combined data on the total yield of delayed neutrons for a broad range of actinides, as compiled in [76]. The data shown for the ^{245}Cm nuclide are complemented with experimental results from Ref. [71] and with DN yields computed within the microscopic approach in [72, 73]. The latter relies on the available data on DN emission probability for some precursor nuclei and on their cumulative yields. The total DN yield for ^{245}Cm, $\nu_d = (0.64 \pm 0.02)\%$, obtained in Ref. [75], is consistent with the fitted value of $(0.621 \pm 0.005)\%$ obtained from the compilation in question.

On the other hand, the ν_d estimates based on summing the precursor contributions [71–73] do not fully agree with the measurements [71] and [75] and among themselves. Understanding the source of this disagreement is important since the summation method is used for estimating the DN characteristics for the nuclides that still await direct measurements. The disagreement between the results obtained by the summation method is probably rooted in different assumptions on the parameters of the charge distribution of fission fragments and on the magnitude of the even–odd effect. Therefore, the measured total DN yield [75] in the fission of ^{245}Cm allows one to estimate the parameters by varying both the computed parameters and the magnitude of the measured even–odd effect in the charge distribution of fission fragments. In its turn, estimating these parameters will allow to clarify the properties of the charge distribution of fission fragments and to evaluate the magnitude of the even–odd effect for the nuclides in the yet-unexplored region of mass and charge.

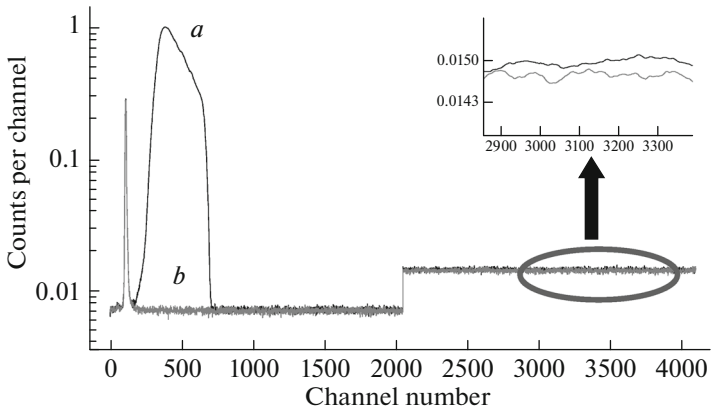

Fig. 16. The apparatus time spectra for the measurements with curium normalized to one reactor burst: *a*—the effect plus background (^{245}Cm), *b*—background only (^{245}Cm with a Cd filter).

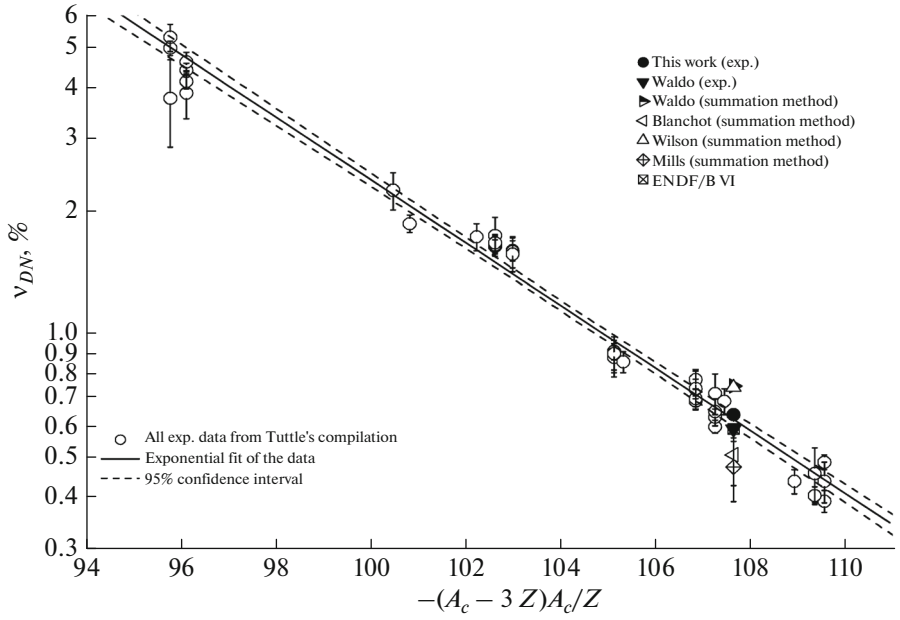

Fig. 17. The compilation [76] supplemented with the DN yield for curium as measured in [75].

9. INVESTIGATIONS OF NUCLEAR FISSION AND RADIATIVE NEUTRON CAPTURE WITH THE n_TOF SOURCE AT CERN

An extensive program of measurements of cross sections for the fission of actinides induced by neutrons over the energy range from the resonance region to 200 MeV was realized in 2001–2007 at CERN [77–84] using the time-of-flight spectrometer n_TOF and a fast multisection ionization chamber constructed and equipped in collaboration with IPPE (Obninsk). Apart from that, the (n, γ) reaction induced by neutrons with energy up to 400 keV was investigated [85–100] using a unique multi-detector spectrometer with total absorption of γ-quanta constructed by the n_TOF Collaboration. All these experiments employed highly enriched targets manufactured at JINR in collaboration with IPPE including the unique sealed targets containing minor actinides for measuring the radiative neutron capture. The data obtained in these experiments have been published in over 20 papers, one of which was submitted in 2015.

REFERENCES

1. I. S. Guseva, G. A. Petrov, A. K. Petukhov, V. E. Sokolov, V. P. Alfimenkov, L. B. Pikelner, and W. I. Furman, "Effective parameters of neutron *p*-wave resonances of ^{233,235}U fission cross section in energy range 1-70 eV", *Proceedings of the ISINN-2 Seminar* (JINR, Dubna, 1994), p. 276.

2. V. P. Alfimenkov, I. S. Guseva, A. M. Gagarski, S. P. Golosovskaya, I. A. Krasnoschokova, A. M. Morozov, G. A. Petrov, V. L. Petrova, A. K. Petukhov, L. B. Pikelner, Yu. S. Pleva, V. E. Sokolov, S. M. Soloviev, and G.V. Val'ski, "*P*-odd, left-right and forward-backward asymmetries of fragment angular distribution in ^{233}U fission induced by the low energy neutrons and forward-backward asymmetry in ^{239}Pu fission", *Proceedings of the ISINN-3 Seminar* (JINR, Dubna, 1995), p. 276.

3. V. P. Alfimenkov, G. V. Val'skii, A. M. Gagarskii, P. Gel'tenborg, I. S. Guseva, I. Last, G. A. Petrov, A. K. Petukhov, L. B. Pikel'ner, Yu. S. Pleve, V. E. Sokolov, V. I. Furman, K. Shrekkenbakh, and O. A. Shcherbakov, "Interference effects in angular distributions of fission fragments in the fission of heavy nuclei induced by thermal and resonance neutrons", Yad. Fiz. **58**, 799 (1995) [Phys. At. Nucl. **58**, 737 (1997)].

4. A. M. Gagarski, I. S. Guseva, S. P. Golosovskaya, I. A. Krasnoschokova, A. M. Morozov, G. A. Petrov, V. L. Petrova, A. K. Petukhov, Yu. S. Pleva, V. E. Sokolov, S. M. Soloviev, G. V. Val'ski, V. P. Alfimenkov, A. N. Chernikov, L. Lason, Yu. D. Mareev, V. V. Novitski, L. B. Pikelner, V. R. Skoy, and M. I. Tsulaya, "Investigations of the parity violation and interference effects in ^{235}U fission induced by resonance neutrons", *Proceedings of the ISINN-5 Seminar* (JINR, Dubna, 1997), p. 182.

5. V. P. Alfimenkov, A. M. Gagarskii, S. P. Golosovskaya, I. S. Guseva, I. S. Krasnoshchekova, L. Lason', Yu. D. Mareev, V. V. Novitskii, G. A. Petrov, V. I. Petrova, A. K. Petukhov, L. B. Pikel'ner, Yu. S. Pleve, V. E. Sokolov, M. I. Tsulaya, and A. N. Chernikov, "Investigations of spatial-parity violation and interference effects in angular distributions of fission fragments in ^{235}U fission induced by resonance neutrons", Yad. Fiz. **63**, 598 (2000) [Phys. At. Nucl. **63**, 539 (2000)].

6. V. P. Alfimenkov, A. N. Chernikov, L. Lason et al., Nucl. Phys. A **645**, 31 (1999).

7. A. M. Gagarski, I. S. Guseva, I. A. Krasnoschokova, G. A. Petrov, V. L. Petrova, A. K. Petukhov, Yu. S. Pleva, V. E. Sokolov, S. M. Soloviev, V. P. Alfimenkov, N. Bazhanov, A. N. Chernikov, W. I. Furman, L. Lason, Yu. D. Mareev, V. V. Novitski, L. B. Pikelner, T. L. Pikelner, A. B. Popov, M. I. Tsulaya, and A. L. Barabanov, "Investigations of parity violation and interference effects in fission of ^{239}Pu induced by resonance neutrons", *Proceedings of the ISINN-10 Seminar* (JINR, Dubna, 2002), p. 184.

8. V. E. Sokolov, A. M. Gagarski, I. S. Guseva *et al., Proceedings of International Conference on Nuclear Data for Science and Technology,* Ed. by R. C. Height et al. (2005), p. 708.

9. A. L. Barabanov, A. B. Popov, and W. I. Furman, "Helicity approach to interference effects in neutron induced fision", *Proceedings of the ISINN-10 Seminar* (JINR, Dubna, 2002), p. 171.

10. A. Barabanov, W. Furman, and A. Popov, in *Astrophysics, Symmetries and Applied Physics at Spallation neutron Sources* (World Scientific, 2002), p. 185.

11. Yu. N. Kopach, A. B. Popov, W. I. Furman, D. I. Tambovtsev, L. K. Kozlovsky, N. N. Gonin, and J. Kliman, "Angular anisotropy of fission fragments from the resonance neutron induced fission of aligned ^{235}U target and the role of $J\pi K$ fission channels", Phys. At. Nucl. **62,** 929 (1999).

12. Yu. N. Kopach, A. B. Popov, V. I. Furman, V. P. Alfimenkov, L. Lason', L. B. Pikel'ner, N. N. Gonin, L. K. Kozlovskii, D. I. Tambovtsev, A. M. Gagarskii, G. A. Petrov, and V. E. Sokolov, "The fission of heavy nuclei induced by resonance neutrons", Fiz. Elem. Chastits At. Yadra **32,** V. 7, 204 (2001) [in Russian].

13. Yu. V. Taran and F. L. Shapiro, "Some methods for polarizing the intermediate-energy neutrons and analyzing their polarization", Zh. Eksp. Teor. Fiz. **44,** 2185 (1963) [in Russian].

14. A. L. Barabanov and W. I. Furman, "New theoretical possibilities of describing *P*-even and *P*-odd angular correlation of fission fragments from resonance-neutron-induced fission", *Proceedings of International Conference on Nuclear Data for Science and Technology,* Ed. By J. K. Dickens (Gatlinburg, Tennessee, 1994), v. 1, p. 448.

15. A. L. Barabanov and W. I. Furman, "Formal theory of neutron induced fission", Z. Phys. A **357,** 411 (1997).

16. A. L. Barabanov and W. I. Furman, "Test of fundamental symmetries as a tool for fission dynamic studies", Czechoslovak Journal of Physics, Suppl. B **53,** 359 (2003).

17. V. M. Strutinskii, "On the angular distribution of fission fragments", Zh. Eksp. Teor. Fiz. **30,** 606 (1956) [in Russian].

18. A. Bohr, "On the theory of nuclear fission," *Proceedings of International Conference on the Peaceful Uses of Atomic Energy* (United Nations Organization, New York, 1956), v. 2, p. 151.

19. J. M. Blatt and L. C. Biedenharn, "The angular distribution of scattering and reaction cross section," Rev. Mod. Phys **24,** 258 (1952).

20. W. Furman and J. Kliman, "Fluctuation of fission characteristics and the structure of fission channels", *Proceedings of the 17^{h} International Symposium on Nuclear Physics,* Ed. by D. Seeliger and H.Kalka (ZfK, Drezden, 1988), p. 142.

21. N. J. Pattenden and H. Postma, "Fission of aligned ^{235}U nuclei induced by neutrons of 0.2 to 2000 eV", Nucl. Phys. A **167,** 225 (1971).

22. National Nuclear Data Center, http://www.nndc.bnl.gov

23. A. L. Barabanov and W. I. Furman, "Particular properties of the $K = 0$ channel in nuclear fission", Yad. Fiz. **72,** 1311 (2009) [Phys. At. Nucl. **72**, 1259 (2009)].

24. S. G. Kadmensky, V. M. Markushev, and W. I. Furman, "Nonconservation of the spin projection to the nucleus symmetry axis in neutron resonances and the Coriolis mixing", Phys. At. Nucl. **35,** 300 (1982).

25. F. Bechvarzh, "Gamma decays of neutron resonances", *Proceedings of the 2nd School on Neutron Physics* (Alushta, 1974), Report JINR D3-7991 (1974), p. 294 [in Russian].

26. V. E. Bunakov and L. B. Pikelner, "Parity and time reversal violation in neutron-nucleus reactions," Progr. Part. Nucl. Phys. **33,** 337 (1997).
27. P. Jesinger, G. V. Danilyan, A. M. Gagarski, P. Geltenbort, F. Goennenwien, A. Koetzle, Ye. I. Korobkina, M. Mutterer, V. Vesvizhevsky, S. R. Neumaier, V. S. Pavlov, G. A. Petrov, V. I. Petrova, K. Schmidt, V. B. Shvachkin, and O. Zimmer, "Interference effect in angular distribution of outgoing particles in ternary fission induced by cold polarized neutrons", Yad. Fiz. **62,** 1723 (1999).
28. K. Schreckenbach, Internal ILL Report 88SCO9T, Grenoble, 1988.
29. V. E. Bunakov and G. A. Petrov, "A possible explanation of the triple correlation origin in ternary fission", *Proceedings of the VIII International Seminar on Interactions of Neutrons with Nuclei,* (JINR, Dubna, 2000), p. 84.
30. A. L. Barabanov, "Spin-orbit interaction in final state as possible reason for *T*-odd correlation in ternary fission", *Proceedings of the IX International Seminar on Interactions of Neutrons with Nuclei* (JINR, Dubna, 2001), p. 93.
31. V. E. Bunakov and S. G. Kadmenskii, "*T*-odd asymmetries of angular distributions of nuclear fragments in ternary fission", Izv. Akad. Nauk, Ser. Fiz. **68,** 1090 (2004) [Bull. Russ. Acad. Sci: Phys. **68,** 1229 (2004)].
32. F. Goennenwein, M. Mutterer, A. Gagarski, I. Guseva, G. Petrov, V. Sokolov, N. Zavarukhina, Yu. Gusev, J. von Kalben, V. Nesvizhavsky, and T. Soldner, "Rotation of compound nucleus ^{236}U in the fission reaction ^{235}U(n,f) induced by cold polarized neutrons", Phys. Lett. B **652**, 13 (2007).
33. G. V. Danilyan, P. Granz, V. A. Krakhotin, F. Mezei, V. V. Novitsky, V. S. Pavlov, M. Russina, P. B. Shatalov, and T. Wilpert, "Rotational effect of fissile nucleus in binary fission of ^{235}U induced by cold polarized neutrons", Phys. Lett. B **679,** 25 (2009).
34. G. V. Danilyan, I. Klenke, V. A. Krakhotin, V. L. Kuznetsov, V. Novitskii, V. S. Pavlov, and P. B. Shatalov, "Prefission gamma-quanta", Yad. Fiz. **72,** 1872 (2009) [Phys. At. Nucl. **72,** 1812 (2009)].
35. G. V. Danilyan, I. Klenke, V. A. Krakhotin, V. V. Novitskii, V. S. Pavlov, and P. B. Shatalov, "Search for *T*-odd correlations in the emission of prompt neutrons in the polarized-neutron-induced fission of ^{235}U nuclei", Yad. Fiz. **73,** 1155 (2010) [Phys. At. Nucl. **73,** 1116 (2010)].
36. G. V. Danilyan, I. Klenke, V. A. Krakhotin, Yu. N. Kopach, V. V. Novitskii, V. S. Pavlov, and P. B. Shatalov, "*T*-odd angular correlations in the emission of prompt gamma rays and neutrons in nuclear fission induced by polarized neutrons", Yad. Fiz. **74,** 697 (2011) [Phys. At. Nucl. **74,** 671 (2011)].
37. G. V. Danilyan, I. Klenke, Yu. N. Kopach, V. A. Krakhotin, V. V. Novitskii, V. S. Pavlov, and P. B. Shatalov, "Effects of rotation of fissioning nuclei in the angular distributions of prompt neutrons and gamma rays originating from the polarized-neutron-induced fission of ^{233}U and ^{235}U nuclei", Yad. Fiz. **77,** 715 (2014) [Phys. At. Nucl. **77,** 677 (2014)].
38. G. A. Petrov, A. M. Gagarskii, I. S. Guseva, V. E. Mokolov, G. V. Vol'skii, A. S. Vorob'eva, D. O. Krinitsin, O. A. Shcherbakov, D. V. Nikolaev, Yu. S. Pleve, V. I. Petrova, and T. A. Zavarukhina, " Major results of an investigation of prompt neutrons from nuclei fission at low excitation energies", Yad. Fiz. **71,** 1165 (2008) [Phys. At. Nucl. **71,** 1149 (2008)].
39. A. M. Gagarski, F. Goennenwein, I. S. Guseva, T. A. Zavarukhina, Yu. N. Kopatch, T. E. Kuzmina, M. Mutterer, V. Nesvizhevsky, G. A. Petrov, T. Soldner, and G. Tiurin, *"T*-odd asymmetry effects of the light particles emission in the heavy nucleus ternary fission by cold polarized neutrons", *Proceedings of the XIX International Seminar on Interactions of Neutrons with Nuclei* (JINR, Dubna, 2011), p. 24.
40. A. L. Barabanov and W. I. Furman, "Fission via compound states and JπK A. Bohr's channels: what we can learn from recent studies with slow neutrons ?", European Physical Journal Web of Conference **21,** 08002 (2012).
41. W. Furman, "Quantum aspects of low-energy nuclear fission", *Proceedings of the Seminar on Fission,* Ed. by C. Wagemans, J. Wagemans, and P. D'hondt (World Scientific, 2010), p. 53.
42. C. E. Porter and R. G. Thomas, "Fluctuations of nuclear reaction widths", Phys. Rev. **104,** 483 (1956).
43. N. Bohr and J. A. Wheeler, "The mechanism of nuclear fission", Phys. Rev. **56,** 426 (1939).
44. V. M. Strutinsky, "Shell effects in nuclear masses and deformation energies", Nucl. Phys. A **95,** 420 (1967) ; "Shells in deformed nuclei", ibid. **122,** 1 (1968).
45. U. Brosa, S. Grossmann, and A. Mũller,"Nuclear scission", Phys. Rep. **197,** 167 (1990).
46. Yu. F. Smirnov and Yu. M. Chuvil'ski, "The structural forbiddenness of the heavy fragmentation of the atomic nucleus", Phys. Lett. B **134,** 25 (1984).
47. C. Wagemans and A. J. Deruytter, "Ratio of the ternary to binary fission cross sections induced by resonance neutrons in ^{235}U", Nucl. Phys. A **194,** 657 (1972).
48. G. S. Ahmadov, Yu. N. Kopatch, S. A. Telezhnikov, F. I. Ahmadov, C. Granja, A. A. Garibov, and S. Pospisil, "Detection of ternary and quaternary fission fragments from ^{252}Cf with a position-sensitive ΔE-E telescope based on silicon detectors", Pis'ma Fiz. Elem. Chastits At. Yadra **12,** 542 (2015).
49. X. Lopart, R. Ballabriga, M. Campbell, L. Tlustos, and W. Wong, "Timepix, a 65k programmable pixel readout chip for arrival time, energy and/or photon counting measurements", Nucl. Instr. Meth. A **581,** 485 (2007).
50. C. Wagemans, "Spontaneous fission", In *Nuclear Fission Process,* Ed. by C. Wagemans (CRC-Press, Boca Raton, 1991).
51. Sh. Zeynalov, F.-J. Hambsch, N. Varapai, S. Oberstedt, and O. Serot, "Prompt fission neutron emission in resonance fission of ^{239}Pu", *Proceedings of the XII International Seminar on Interaction of Neutrons with Nuclei* (JINR, Dubna, 2004), E3-2004-169, pp. 371–379.

52. C. Budtz-Jorgensen and H. -H. Knitter, "Simultaneous investigation of fission fragments and neutrons in ^{252}Cf(Sf)", Nucl. Phys. A **490,** 307 (1988).

53. F.-J. Hambsch, H.-H. Knitter, C. Budtz-Jorgensen, and J. P. Theobald, "Fission mode fluctuation in the resonances of ^{235}U(*n,f*)", Nuclear Physics A **491,** 56 (1989).

54. Sh. S. Zeinalov, M. Florek, W. I. Furman, V. A. Kriatchkov, and Yu. S. Zamyatnin, "Neutron energy dependence of ^{235}U(*n,f*) mass and TKE distributions around 8.77 eV resonance", *Proceedings of the VII International Seminar on Interaction of Neutrons with Nuclei* (JINR, Dubna, 1999), E3-1999-212, pp. 258–262.

55. Sh. S. Zeinalov, M. Florek, W. I. Furman, V. A. Kriachkov, and Yu. S. Zamyatnin, „Neutron Energy Dependence of Fission Fragment Mass & TKE Distributions of ^{235}U(*n,f*)- Reaction Below 10 eV", *Proceedings of the 4th International Conference on Dynamical Aspects of Nuclear Fission* (Casta-Papiernicka, Slovak Republic), Ed. by J. Kliman (World Scientific, Singapore, 2000, pp. 417–423).

56. Sh. Zeinalov, W. Furman, and F. -J. Hambsch, "Investigation of mass-TKE distributions of fission fragments from ^{235}U(*n,f*) reaction in resonances", *Proceedings of the XIII International Seminar on Interaction of Neutrons with Nuclei* (JINR, Dubna, 2006), E3-2006-7, pp. 351–359.

57. H. Takahashi, T. Kurahashi, L. Zhang, D. Fukuda, M. Nakazawa, and M. Misawa, "Digital signal processing for CdTe detectors based on a waveform clustering algorithm", Nucl. Instr. Meth. A **458,** 375–381 (2001).

58. W. K. Warburton and P. M. Grudberg, "Current trends in developing digital signal processing electronics for semiconductor detectors", Nucl. Instr. Meth. A **568,** 350-358 (2006).

59. G. Pasquali, R. Ciaranfi, L. Bardelli, M. Bini, A. Boiano, F. Giannelli, A. Ordine, and G. Poggi, "A DSP equipped digitizer for online analysis of nuclear detector signals", Nucl. Instr. Meth. A **570,** 126–132 (2007).

60. G. Gerardi, L. Abbene, A. La Manna, F. Fauci F, and G. Raso, "Digital filtering and analysis for a semiconductor X-ray detector data acquisition", Nucl. Instr. Meth. A **571,** 378–380 (2007).

61. O. Zeinalova, Sh. Zeinalov, F.-I. Khambsh, and S. Oberstedt, "Application of the methods of digital signal processing in nuclear spectroscopy", Izv. Acad. Nauk, Ser. Fiz. **73,** 533–539 (2009) [in Russian].

62. C. E. Shannon, "A mathematical theory of communication", The Bell System Technical Journal **27,** 379–423 (1948); *ibid*. **27,** 623–656 (1948).

63. Sh. S. Zeynalov, O. V. Zeynalova, and V. I. Smirnov, "Delayed neutron yield measurement on thermal neutron induced fission of ^{237}Np using cross-correlation technique", in *Nuclear Physics and Atomic Energy 2006-2009*, v. 10, No. 1, pp. 100–104.

64. A. Andreev, D. Bogdanov, V. Chepigin, V. Gorshkov, K. Michailov, A. Kabachenko, G. Popeko, S. Saro, G. Ter-Akopian, A. Yeremin, and Sh. Zeinalov, "4-π ionization chamber–a detector for a kinematic separation of heavy ion reaction products", Nucl. Instr. Meth. A **330,** 209–220 (1993).

65. O. V. Zeinalova, Sh. S. Zeinalov, F. I. Khambsh, and S. Oberstedt, "A twin position-sensitive ionization chamber for implementing the backgammon and time-projection methods", Izv. Akad. Nauk, Ser. Fiz. **75**, 1623–1628 (2011) [in Russian].

66. G. R. Keepin, *Physics of Nuclear Kinetics (*Addison-Wesley Reading, 1965).

67. R. J. Tuttle, "Delayed neutron data for reactor physics analysis", Nucl. Sci. Eng. **56,** 37 (1975).

68. G. D. Spriggs, J. M. Campbell, and V. M. Piksaikin, "A method for determining the intensity of concomitant neutron source D(*d, n*)^{3}He when studying the characteristics of delayed neutrons from nuclear fission induced by neutrons from reaction T(*d, n*)^{4}He", LANL report LA-UR-98-1619, Rev. 3 (Los Alamos, 1999).

69. S. B. Borzakov, E. Dermendzhiev, Yu. S. Zamyatnin, V. M. Nazarov, S. S. Pavlov, A. D. Rogov, and I. Ruskov, "A facility for studying the delayed neutrons and preliminary determination of B_{eff} for ^{233}U with respect to ^{235}U", Atomnaya Energiya **79,** 231 (1995) [in Russian].

70. S. B. Borzakov, A. N. Andreev, E. Dermendjiev, A. Filip, W. I. Furman, Ts. Panteleev, I. Ruskov, Yu. S. Zamyatnin, and Sh. Zeinalov, "Measurements of delayed-neutron yields from thermal-neutron-induced fission of ^{235}U, ^{233}U, ^{239}Pu, and ^{237}Np",Yad. Fiz. **63,** 589 (2000).

71. R. W. Waldo, R. A. Karam, and R. A. Meyer, "Time dependent measurements and a predictive model", Phys. Rev. C **23,** 3 (1981).

72. R. Mills, M. F. James, and D. R. Weaver, "Study of the delayed neutron yield and its time dependence", *Proceedings of International Conference on Nuclear Data for Science and Technology* (Julich, 13–17 May 1991), pp. 86–88.

73. W. B. Wilson and T. R. England, "Delayed neutron study using ENDF/B-VI basic nuclear data", Progress in Nuclear Energy **41,** 71–107 (2002).

74. N. A. Gundorin, K. V. Zhdanova, V. E. Zhuchko, L. B. Pikel'ner, N. V. Rebrova, I. M. Salamatin, V. I. Smirnov, and V. I. Furman, "A measurement of the delayed-neutron yield from ^{237}Np fission induced by thermal neutrons"," Yad. Fiz. **70,** 1011 (2007) [Phys. At. Nucl. **70,** 975–982 (2007)].

75. V. R. Andrianov, V. I. Vyachin, N. A. Gundorin et al., "The yield of delayed neutrons in the thermal-neutron-induced reaction ^{245}Cm(*n,f*)", Yad. Fiz. **71,** 1705 (2008) [Phys. At. Nucl. **71,** 1675–1683 (2008)].

76. V. M. Piksaikin, S. G. Isaev, and A. A. Goverdovsky, "The yield of delayed neutrons in the reaction ^{245}Cm(*n,f*) induced by thermal neutrons", Progress in Nuclear Energy **41,** 361 (2002) [in Russian].

77. M. Calviani, J. Praena, U. Abbondanno, and the n_TOF Collaboration, "High-accuracy ^{233}U(n,f) cross-section measurement at the white-neutron source n_TOF from near-thermal to 1 MeV neutron energy", Phys. Rev. C **80,** 044604 (2009).

78. C. Paradela, L. Tassan-Got, L. Audouin, and the n_TOF Collaboration, "Neutron-induced fission

cross section of U-234 and Np-237 measured at the CERN Neutron Time-of-Flight (n_TOF) facility", Phys. Rev. C **82,** 034601 (2010).

79. D. Tarrío, L. Tassan-Got, L. Audouin, and the n_TOF Collaboration, "Neutron-induced fission cross section of Pb-nat and Bi-209 from threshold to 1 GeV : An improved parametrization", Phys. Rev. C **83,** 044620 (2011).

80. M. Calviani, M. H. Meaze, N. Colonna, and the n_TOF Collaboration, "Neutron-induced fission cross section of Cm-245: New results from data taken at the time-of-flight facility n_TOF", Phys. Rev. C **85,** 034603 (2012).

81. F. Belloni, P. M. Milazzo, M. Calviani, and the n_TOF Collaboration, "Neutron-induced fission cross section measurement of U-233, Am-241 and Am-243 in the energy range 0.5 MeV <= E-n <= 20 MeV at n_TOF at CERN", Physica Scripta **150,** 014005 (2012).

82. R. Sarmento, M. Calviani, J. Praena, and the n_TOF Collaboration, "Measurement of the U-236(*n*,*f*) cross section from 170 meV To 2 MeV at the CERN n_TOF facility", Phys. Rev. C **84,** 044618 (2011).

83. M. Calviani, S. Andriamonje, E. Chiaveri, and the n_TOF Collaboration, "Fission cross-section measurements of U-233, Cm-245 and Am-241, Am-243 at CERN n_TOF facility", Journal of the Korean Physical Society **59,** 1912–1915 (2011).

84. F. Belloni, M. Calviani, N. Colonna, and the n_TOF Collaboration, "Neutron-induced fission cross-section of U-233 in the energy range 0.5 < E-n < 20 MeV", Eur. Phys. J. A **47,** 160 (2011).

85. C. Guerrero, D. Cano-Ott, E. Mendoza, and the n_TOF Collaboration, "Measurement and resonance analysis of the Np-237 neutron capture cross section", Phys. Rev. C **85,** 044604 (2012).

86. G. Tagliente, P. M. Milazzo, K. Fujii, and the n_TOF Collaboration, "Neutron capture on Zr-94 : Resonance parameters and Maxwellian-averaged cross sections", Phys. Rev. C **84,** 014607 (2011).

87. C. Lederer, N. Colonna, C. Domingo-Pardo, and the n_TOF Collaboration, "Au-197(*n,* gamma) cross section in the unresolved resonance region", Phys. Rev. C **83,** 034608 (2011).

88. D. Cano-Ott, F. Alvarez-Velarde, E. Gonzalez-Romero, and the n_TOF Collaboration, "Neutron capture measurements on minor actinides at the n_TOF facility at CERN : Past, present and future", Journal of the Korean Physical Society **59,** 1809–1812 (2011).

89. M. Mosconi, K. Fujii, A. Mengoni, and the n_TOF Collaboration, "Neutron Physics of the Re/Os clock. I. Measurement of the (n, γ) cross sections of Os-186, Os-187, Os-188 at the CERN n_TOF facility", Phys. Rev. C **82,** 014607 (2010).

90. K. Fujii, M. Mosconi, A. Mengoni, and the n_TOF Collaboration, "Neutron physics of the Re/Os clock. III. Resonance analyses and stellar (n, γ) cross sections of Os-186, Os-187,Os-188", Phys. Rev. C **82,** 015804 (2010).

91. C. Massimi, C. Domingo-Pardo, G. Vannini, and the n_TOF Collaboration, "Au-197(n, γ) cross section in the resonance region", Phys. Rev. C **81,** 044616 (2010).

92. C. Guerrero, U. Abbondanno, G. Aerts, and the n_TOF Collaboration, "The n_TOF total absorption calorimeter for neutron capture measurements at CERN", Nucl. Instr. Meth. A **608,** 424–433 (2009).

93. C. Domingo-Pardo, U. Abbondanno, G. Aerts, and the n_TOF Collaboration, "The measurement of the 206Pb(n, γ) cross section and stellar implications", Journal of Physics G **35,** 014015 (2008).

94. R. Terlizzi, U. Abbondanno, G. Aerts, and the n_TOF Collaboration, "The La-139($n,$ γ) cross section : Key for the onset of the *s*-process", Phys. Rev. C **75,** 034603 (2007).

95. F. Gunsing, U. Abbondanno, G. Aerts, and the n_TOF Collaboration, "Status and outlook of the neutron time-of-flight facility at CERN", Nucl. Instr. Meth. B **261,** 925–929 (2007).

96. C. Domingo-Pardo, U. Abbondanno, G. Aerts, and the n_TOF Collaboration, "Measurement of the neutron capture cross section of the *s*-only isotope Pb-204 from 1 eV to 440 KeV", Phys. Rev. C **75,** 014601 (2007).

97. C. Domingo-Pardo, U. Abbondanno, G. Aerts, and the n_TOF Collaboration, "Measurement of the radiative neutron capture cross section of Pb-206 and its astrophysical implications", Phys. Rev. C **76,** 044610 (2007).

98. C. Domingo-Pardo, U. Abbondanno, G. Aerts, and the n_TOF Collaboration, "New measurement of neutron capture resonances in Bi-209", Phys. Rev. C **74,** 024608 (2006).

99. G. Aerts, U. Abbondanno, H. Alvarez, and the n_TOF Collaboration, "Neutron capture cross section of Th-232 measured at the n_TOF facility at CERN in the unresolved resonance region up to 1 MeV", Phys. Rev. C **73,** 054605 (2006).

100. G. Tagliente, K. Fujii, P. M. Milazzo, and the n_TOF Collaboration, "Neutron capture cross section of ^{90}Zr: Bottleneck in the *s*-process reaction flow", Phys. Rev. C **77,** 034603 (2008).

Translated by A. Asratyan